2022

Y-Chromosome DNA Extraction from Post-Cranial Skeletal Elements

Mykala D. Ward
University of Montana, Missoula

Y-CHROMOSOME DNA EXTRACTION FROM POST-CRANIAL SKELETAL ELEMENTS

By

MYKALA DENISE WARD

Bachelor of Arts, Texas Tech University, Lubbock, TX, 2020

Thesis

Presented in partial fulfillment of the requirements
for the degree of

Master of Arts
In Anthropology, Forensic Anthropology

The University of Montana
Missoula, MT

May 2022

Approved by:

Scott Whittenburg,
Graduate School Dean

Dr. Meradeth Snow, Chair
Anthropology

Dr. Randall Skelton
Anthropology

Dr. Mark Heirigs
Sociology

Ward, Mykala, M.A., Spring 2022 Anthropology

Y-Chromosome DNA Extraction from Post-Cranial Skeletal Elements

Chairperson: Dr. Meradeth Snow

Abstract

The use of DNA in forensic science has become an integral tool for victim and perpetrator identifications, missing person's cases, paternity testing, etc. A major use of DNA is in the identification of unknown deceased individuals. With a reported number of individuals well over 8,000 in the United States, improved methods to accurately collect and analyze DNA from modern human bone are needed.

This project took the preliminary steps to improve DNA sampling and extraction methods by analyzing the Y-chromosome DNA yield from the two bone types. While both types are composed of the same materials, cortical bone is the tightly packed bone on the outer layer, and trabecular is the sponge-like bone located inside. The yields observed in cortical and trabecular bone samples in a set of human remains could help determine what type of samples need to be taken for successful DNA analysis. Samples were collected from various locations throughout the skeleton from each of the two bone types and subjected to quantitative polymerase chain reaction (qPCR) analysis. qPCR determines the amount of DNA in each sample. The averages from each bone type were compared to determine if one type preserves DNA better.

The preliminary data collected from this project has provided a stepping stone in the right direction to improve how DNA sampling from modern human remains is done. Further research on this topic must be done to increase the validity of the results and affect the current methods used.

Acknowledgments

First, I would like to give my thanks and appreciation to my mentor and research partner, Keith Biddle. Without his guidance, support, and ideas, this project would not have been possible. Next, I would like to thank my committee chair and advisor, Dr. Meradeth Snow. Her constant guidance and support whenever I needed it gave me the ability to successfully finish this project even when everything seemed to go wrong. I would also like to thank my family for believing in me and supporting me in everything I do.

Lastly, I would like to thank David Smith and his next of kin. While David could not give his direct permission, the use of his remains was the most crucial part of this project. Without having a complete set of remains to analyze, the data would have lacked validation. Thank you to David's next of kin for allowing us to continue our project and the donation of David's remains to the University of Montana Forensic Anthropology Collection.

Table of Contents

List of Figures

List of Tables

1.0 Introduction

DNA has become an integral part of modern forensic science (Roewer 2013). It is used in many scenarios such as crime scene investigations, victim and perpetrator identifications, missing person's cases, paternity testing, etc. A major use of DNA is for the identification of unknown individuals. Tissue and blood are the main types of material used for DNA analysis but are not always available. In the case that only bones are recovered, the bone itself must be used. An issue with this is a lot of medical examiners don't know how and where to get DNA from skeletal elements that would provide the best results for identification.

DNA methods and technologies are constantly being improved but methods on how and where to sample DNA are lacking. Little to no research has been done on specific locations on the bones and different bone types in terms of DNA yield. Some of the only articles available don't discuss techniques to collect samples nor discuss where a sample should be taken from to yield the best DNA sample. Research and improved methods regarding the collection of bone for the identification process is needed to bridge the gap between the unknown remains and the person they belong to.

The goal of this project is to analyze the Y-chromosome DNA yield from the two different bone types, cortical and trabecular. Each type of bone, while made of the same material, have different structural properties, and therefore could preserve DNA in different ways. Currently no research has been done in the modern context on human remains that test the difference in DNA yield based on bone types. If one type of bone does give better results, only using that type in future testing could help reduce random sampling. Random sampling of the remains could waste time, money, resources, and even the remains themselves. Minimizing

testing will reduce damage inflicted on the bones from taking samples and improve the condition of the bones when being returned to their families.

The suspected outcome of this project is to create a steppingstone in research on improving methods for DNA sampling from modern human bones. With the information gained from this project more research could be done to further improve methods and allow for crime labs and police departments to have better success in testing DNA samples.

1.1 Hypothesis

Due to the structure of trabecular bone, samples taken throughout the remains that contain only the trabecular bone will yield higher amounts of Y-Chromosome DNA molecules in comparison to samples taken from the compact bone.

To support this, the results would need to show that at each skeletal location, and overall, the trabecular bone samples had a higher yield in ng/µl of the Y-Chromosome DNA. The sponge like structure of the trabecular bone provides more surface area for the various bone cells, and their associated DNA, to accumulate. The location of the trabecular bone is also a factor that could affect the preservation of DNA. With the trabecular bone being encased within the hard cortical bone, it does not have the same exposure to taphonomic processes and contamination that might affect the cortical bone's DNA preservation.

2.0 Literature Review

2.1 The Introduction of DNA Analysis in Forensic Science

The first use of DNA in a forensic context happened in Leicester, England, in the late 1980s (Napper 2000). In 1983 a 15-year-old girl named Lynda Mann was raped and murdered; then, in 1986, 15-year-old Dawn Ashworth was raped and murdered less than a mile from Mann's crime scene. The similarities in the cases caused police to link them, but they had no idea who committed these heinous crimes. At this time, DNA was a new method that had yet to be used in a criminal case. The police wanting to try everything to catch their killer, contacted a professor from the local university who was working on DNA analysis for diseases. A dragnet was used to collect DNA samples from men in nearby villages, which resulted in over 6000 samples being collected. While the dragnet missed the killer because he paid someone to test for him, the proxy was found and led the police straight to the killer, Colin Pitchfork. A DNA test from Pitchfork confirmed the match to samples left on the scene and allowed for a conviction of both murders resulting in two life sentences (Napper 2000). This case, and its novel use of DNA to find a murderer, spurred a movement in the world of forensic DNA.

The use of forensic DNA testing and analysis spread across the world very quickly. With the quick spread also came the need for an organized system to avoid conducting dragnets like seen in the Pitchfork case (Rothstein and Talbott 2006). Around the world, over 60 countries have created their own government-based forensic DNA database, and worldwide there are over 125 million offender profiles in these databases (Ge and Budowle 2021). The United States joined the movement and created the Combined DNA Index System (CODIS), a database of DNA profiles taken from suspects, victims, family members, and felons entering into the prison system (Adams 2002; Hares 2012; “CODIS and NDIS Fact Sheet” n.d.; Rothstein and Talbott

2006; Miller, Brown, and Budowle 2003). The pilot of CODIS was introduced in 1990 and formally established in 1994, containing three levels of hierarchy: local, state, and federal (known as the National DNA Index System or NDIS). In the beginning, CODIS only had samples from individuals, both victims and suspects, of current cases and quickly grew to include family members and individuals required to give samples due to crimes they have committed. Legislation has been passed that requires all inmates convicted of a felony must provide their DNA to CODIS. This law, when enacted, solved many cold cases that had DNA but no suspects.

To compare DNA samples, scientists have to look at specific portions of the DNA called STRs or short tandem repeats (Wyner, Barash, and McNevin 2020). These sections in the human genome contain three to six basepairs that repeat side by side. The number of times the section repeats is inherited from the parents of an individual. STRs are highly variable between individuals, meaning that the number of repeats at each locus varies from person to person, allowing them to be used in identification. The probability of the number of repeats that occur in the population is used to confirm the validity of the results by calculating the probability of having a certain repeat motif in comparison to the population at large (Wyner, Barash, and McNevin 2020). These STRs are what CODIS uses to compare DNA profiles.

The number of STRs used in the system has increased since the database's start in 1997 (Miller, Brown, and Budowle 2003; Hares 2012; Wyner, Barash, and McNevin 2020). Starting with 13 from 1997, CODIS currently recognizes 20 STR loci used to identify individuals. The use of the 20 markers was officially implemented beginning January 1, 2017. In mid-2009, NDIS started to consider expanding the system with recommendations from the Scientific Working Group on DNA analysis methods and the FBI issued standards for Quality Assurance (QAS) for

Forensic DNA Testing and Databasing Laboratories (Hares 2012). In May of 2010, the FBI created the CODIS Core STR loci Working Group to look at the existing STR loci and investigate if adding more to the original 13 would be beneficial or if any current STR loci need to be removed. This group first created guidelines to determine what STR loci can be used in analyses. The Working Group then went to major DNA testing kit manufacturers to obtain insight into potential STR loci that could be added (Hares 2012). This group is responsible for how the analysis of DNA in forensics is consistent and as reliable as it is today.

As mentioned before, the STR loci analyzed in the CODIS database must follow guidelines to be considered. To determine what markers are used, researchers use specific criteria. These include: the DNA marker cannot have any links to medical condition or defects, each marker must have a mutation rate of 0.3% or less, must have high discrimination (high variability between individuals), can have widespread use (can be used in any accredited lab), and complies with FBI quality standards (Hares 2012). Even from the beginning, laws and regulations were passed to ensure that any markers used could not be linked to physical traits such as hair or skin color (Wyner, Barash, and McNevin 2020).

The primary type of DNA used in all current databases is autosomal. Every individual has unique autosomal DNA STRs that are the best to use for identification, but research on Y-chromosome STRs has shown that their use in forensic DNA analysis can be just as beneficial (Roewer 2019; Wyner, Barash, and McNevin 2020). Y-chromosome STRs have been used in forensics almost as long as autosomal, but due to its patrilineal inheritance, it has not been studied as much (Kayser 2017; Quintana-Murci and Fellous 2001). With the increase in known Y-STR loci, Y-chromosome analysis is being used more and more.

2.2 The Y-chromosome

The Y-chromosome is the male sex chromosome located within the 23rd pair of chromosomes in human DNA. It is comprised of approximately 57 million base pairs and is only present in biologically male individuals (Quintana-Murci and Fellous 2001). The chromosome was first successfully mapped in 1986 by Vergnaud at the Pasteur Institute in France. The Y-chromosome is only passed on from fathers to sons. Its unilateral inheritance has created a view that it is not as valuable in forensics as autosomal DNA (Kayser 2017; Siegert, Roewer, and Nothnagel 2015; D'Amato, Bajic, and Davison 2011; Roewer 2019; Quintana-Murci and Fellous 2001). While it does not carry as strong has a role as autosomal DNA in the forensics world, the Y-chromosome has proven to help solve cases involving male individuals when an autosomal test is not informative enough.

One of the first instances of its use was in Germany in 1990 (Roewer 2019). A highly publicized murder of a woman killed after engaging in consensual intercourse with the perpetrator. To find the perpetrator, DNA was collected from the victim and tested. The standard DNA techniques failed to yield a result due to the comingling of DNA from the victim and perpetrator. Polymerase chain reaction (PCR) analysis was done for recently developed STR markers to combat this issue, one being located on the Y-chromosome. The amplification of the sample showed the Y-chromosome STR was successfully amplified and gave the investigators something to work with to identify the perpetrator (Roewer 2019). Using only information from the Y-chromosome had not yet been used in forensics. In this case, the Y-chromosome DNA gave evidence that it can be used in many field contexts that were initially not recognized. Recently the Sexual Assault Forensic Evidence Reporting (SAFER) working group published a

report about the best practices for sexual assault kits that recommends that after initial autosomal testing, to then do a secondary test for Y-STRs (Roewer 2019).

2.2.1 Current Uses

The Y-chromosome has gained popularity in forensic applications in the last 10-15 years. Research on possible uses and methods has increased due to this popularity. Like autosomal DNA, specific STR loci are analyzed to match samples from an unknown individual to a known sample (Kayser 2017; Ballantyne et al. 2014). Over the last ten years, approximately 21 different STR loci have been identified as having the variability needed between related individuals to be ideal for use in forensic context for identification purposes (Ballantyne et al. 2014; Kasu et al. 2019; D'Amato, Benjeddou, and Davison 2009; D'Amato et al. 2010). Like the guidelines for CODIS, there are ones similar for finding STR loci on the Y-chromosome. Like the autosomal STR markers, Y-chromosome markers have varying mutation rates, discrimination between individuals, and lack links to diseases. The increasing use of the Y-chromosome in forensic cases has increased the need for these guidelines.

The primary use of Y-chromosome DNA analysis is in sexual assault and rape cases where the victim is female and the perpetrator is male. When samples are taken from female victims, the higher volume of the female's DNA overrides the perpetrator's in the sample (Roewer 2019). The mixed sample makes it hard to create a profile from the autosomal DNA, but analyzing the Y-chromosome may have better results because only the perpetrator has it. Running a test that only amplifies Y-STRs is the most reliable way to ensure the victim's DNA doesn't contaminate the perpetrators.

In addition to its primary use in assault and rape cases, the Y-chromosome has also been advantageous in other situations such as plane crashes, mass grave excavations, missing person cases, etc. (Kayser 2017; Siegert, Roewer, and Nothnagel 2015). When multiple male family members are either in a suspect pool, involved in an accident or suspected of being buried in a mass grave, testing for the Y-chromosome can be helpful. Analyzing the Y-chromosome DNA present not only confirms the biological sex of the individual but can differentiate and link families. Using the highly variable STR loci that have been discovered, investigators can see if the individuals are related and to what extent this relation is, an example being if the individuals are father and son, or brothers, or a more distant relation (Roewer 2019; Kayser 2017).

To use the Y-chromosome in a way that helps identify an individual or match a known sample, the data produced must go through statistical processes just like the autosomal samples (Andersen et al. 2015). These analyses determine the probability of the specific Y-STR profile matching an individual. After a DNA sample has been analyzed and a match has potentially been found, the analyst must calculate the match's probability. This is where population databases are helpful. Each STR allele from the sample is compared to a random selection of individuals in the database. The probability of how many individuals have that repeat is calculated. After all the alleles have gone through that process, the probability of those occurring together is calculated. This final probability is used in court to prove a match or non-match, or, more accurately, the probability of the two DNA sources coming from the same source (Andersen et al. 2015; Science 1992).

The Discrete Laplace method is what is primarily used to achieve this in Y-chromosome analyses. This method uses a model population representing actual populations (Andersen et al. 2015). A model population is used due to the lack of full population representation in databases

(Andersen et al. 2015). The data in the model is derived from available populations but fills in the missing holes they contain. Discrete Laplace estimates the probability of a given sample having the number of repeats at each locus based on the model population. This process is primarily done using software created by Andersen and Eriksen that makes the comparisons once samples are entered (2019). The software is designed to compare samples to the model population and determine the probability without having to do it all by hand (Andersen et al. 2015). This information is what is used to determine a potential ancestral population. The number of repeats at one locus can be common, but the combination of all of them together is rare.

Since the realization of its usability to help identify unknown individuals, using Y-chromosome DNA profiles can sometimes cause issues when presented in court (Roewer 2019; Andersen and Balding 2017). Due to immediate family members having almost identical Y-chromosome DNA, when presented, the defense could try and argue that the sample could be that of a family member and not of the defendant. Although that is true, when using data collected from Y-STRs, a match is statistically analyzed and shows the accuracy of the match (Ballantyne et al. 2014; Roewer 2019; Andersen and Balding 2017; Andersen et al. 2015). An example of this happened in 2015 in Germany. The prosecution presented Y-chromosome DNA evidence that matched the defendant in the case. The defense tried to argue that they could not make an individual identification with the Y-chromosome DNA like they could with autosomal. Due to the statistical analysis, the DNA was a match, and the highest German court agreed. This caused them to make clear guidelines that explain Y-STR use in court cases (Roewer 2019). The increasingly prevalent use of Y-chromosome DNA in forensic applications has created the need for more research, increasing the accuracy and usefulness of analyzing it. Even with the ability to

accurately identify an individual based on their Y-chromosome DNA alone, it is commonly used with other DNA analyses (Roewer 2019).

In many cases, DNA samples collected from crime scenes, from unidentified bodies, or victims have nothing to be compared to for identification purposes. However, the Y-chromosome DNA of male individuals can be analyzed to infer the individual's paternal bio-geographical origin to possibly help narrow down the pool of possible individuals (Roewer 2019). The process uses variable DNA regions that have minor changes between generations but significant differences between familiar lines (Syndercombe Court 2021). Bio-geographical tracing analyzes haplotype frequencies to infer the source of the paternal line of ancestry using a phylogenetic tree. Phylogenetic trees show lineages traced back to common ancestors and can be used in many contexts. The sample can be compared to other individuals to establish relationships and therefore show origins (Syndercombe Court 2021).

The first notable use of phylogenetic trees in a forensic context was during the height of the AIDS epidemic (Siljic et al. 2017). To identify the origin of transmission of the AIDS virus, its DNA was genetically traced from person to person. Each time it was transmitted from one person to the next, there was a slight variation. The locus of mutation is different between different groups so that it can be traced. The tracing of linkage used for the AIDS virus is the same process used for haplotype frequencies using Y-chromosome DNA (Syndercombe Court 2021). This method was used to identify an unknown person in 2000 in Poland (Roewer 2019). A serial rapist was on the loose, but no suspects could be identified. DNA was left on victims, but the samples were comingled. With no database matches from using autosomal DNA, investigators turned to the Y-chromosome. The sample was compared to a dragnet of 11,000 male volunteers. One individual tested was matched to the Y-chromosome sample, but when

compared to the autosomal DNA for confirmation, the sample did not match. These results concluded that this individual was a family member of the perpetrator. After looking through his family tree, the brother of the volunteer was revealed to be the perpetrator (Roewer 2019). This analysis was conducted 22 years ago when research on the subject was in its infancy. Current research has dramatically improved and continues to improve the methods and accuracy.

Haplotype searching can be done with high precision due to a robust phylogenetic tree created from the Y-Chromosome STR Haplotype Reference Database (YHRD) (Rothstein and Talbott 2006; Roewer 2019). The YHRD is comprised of reference DNA samples from anonymous individuals from around the world from a multitude of datasets. Over time researchers have compiled thousands of samples to create a way to compare and trace lineages (Syndercombe Court 2021; Roewer 2019). Haplotyping cannot pinpoint and identify specific people but can narrow down the suspects. Further investigation can be done from the initial haplotype search to find a surname associated with decedents of certain genetic lines (Rothstein and Talbott 2006). Surname searching is a complex and novel method with similar ideas to familial DNA searches.

2.2.2 Ethical Concerns

All fields of study involving humans can run into ethical concerns and must consider these when conducting research. Not everyone will agree with how a study is conducted or how the people involved are treated, but there should be a basic understanding of what is ethical and what is not. In studying DNA, especially in a modern context, the main concern is how samples are collected and what is done with them once they are.

Using methods such as haplotyping in a forensic case creates possible ethical concerns in searching a family for a match to an unknown sample (Syndercombe Court 2021). This is one of the main issues that is seen currently. The use of familial matching was not largely known, so there were no significant concerns from the public until 2018, when Joseph DeAngelo was identified as the Golden State Killer using a familial DNA search (Phillips 2018). While identifying GSK was not the first use of forensic genealogy, the severity of the crimes, mixed with the 30 years of searching done to identify him, created a media storm. The case's publicity introduced people to this method and how DNA could be used, producing concerns about the possible misuse (Phillips 2018). The issue that arose in this case concerned using a public ancestry tracing site and whether it was ethical to use it without direct permission from the individuals using it.

Another high-profile case that used familial DNA tracing was identifying the Boston Strangler (Syndercombe Court 2021). Albert DeSalva admitted to the crimes before his death, but no physical evidence could link him to the crime. To put the case to rest, investigators collected a discarded water bottle used by DeSalva's nephew and tested the Y-chromosome DNA to see if it matched the crime scenes. The test proved successful, but the nephew felt violated since he did not consent to have his DNA tested (Syndercombe Court 2021). In the United States and other countries, DNA can be collected from discarded items. These include gum, cigarettes, or food items. While the DNA collected is non-admissible in court, it provides enough evidence for investigators to obtain a warrant to collect a sample directly from a suspect. This happened in the Golden State Killer case and many notable others. When investigators locked in on DeAngelo, they collected his trash after he had put it into a public garbage can and tested the DNA present. The DNA matched the DNA on file from the victims, so the investigators were

able to get a warrant for his arrest and a more reliable test. Cases like the DeSalva case caused the United Kingdom to criminalize all nonconsensual DNA collection, including discarded items, in 2006 (Syndercombe Court 2021). While this concern is primarily when searching for a killer or another criminal suspect, it can apply to missing and unclaimed bodies.

An example of this could be if an individual were placed up for adoption as an infant. As an adult, that individual dies and can't be identified. If the biological family did not want to have any contact or did not know about the individual, familiar tracing and linking could create problems with the biological family. While this is not something that would often happen, considering these issues must be done.

In addition to familial connections using haplotyping, racial discrimination can cause problems. The possible bias of an individual may come into play for investigators. If the haplotyping traces an individual to African ancestry, which can lead to an assumption of skin color, investigators may overlook individuals who don't match their assumption (Syndercombe Court 2021). This happened in The Netherlands in 1999 after the murder of Marianne Vaastra (Syndercombe Court 2021; Kayser 2017). The brutality of her murder made the local villagers lay blame on asylum seekers in the area based on their idea that the non-European immigrants were below them and 'primal.' The racial prejudice against these people biased the investigation, leading investigators to waste time and money looking at the asylum seekers with no supporting evidence. Later, haplotype analysis was done with the perpetrator's Y-chromosome DNA, resulting in possible Northwestern European descent (Syndercombe Court 2021; Kayser 2017). The time wasted on looking at the asylum seekers could have been used to find the killer and not create more racial tension in the area.

In identifying remains, if investigators are told the individual might be of African origin/decent, any missing person that does not fit the stereotypical look will be eliminated. If the physical attribute of the individual differs from the preconceived look, the correct person will be overlooked, and a positive ID wouldn't be made. Not only does this support racial profiling, but a human would remain nameless and leave families still wondering what happened to their loved ones.

2.3 Using the Y-chromosome to Identify Skeletal Remains

Hundreds of thousands of people are considered missing or unidentified worldwide, and this number increases every day. In the United States alone, the National Crime Information Center (NCIC) reported 90,000 missing persons and over 8,000 unidentified individuals as of 2020 (“2020 NCIC Missing Person and Unidentified Person Statistics” 2020). These numbers increase every year without much resolution to the already open cases. DNA is the most reliable and the quickest solution for identifying remains. In the modern world, most countries have a way to access DNA testing facilities and DNA databases to help identify unknown remains (Parsons et al. 2019). The increased use of DNA analysis in forensics has made it a more easily accessible resource. While not every crime lab or medical examiner's office contains a DNA lab, nationally recognized labs have been established to do testing for them.

When testing DNA to identify skeletal remains, like most other DNA tests, having a complete STR profile is the best. Getting a full STR profile is not always possible with bone sampling, and having the complete profile doesn't mean you have an identification. Just like in criminal cases, a comparison to a reference sample has to be made (Parsons et al. 2019). If a person has been reported missing, their biological relatives usually give either a sample of their DNA or something that has the missing person's DNA. If a person has not been reported as

missing, identification through comparison can be challenging (Parsons et al. 2019; Kayser 2017). If the remains don't have a suspected identification, other methods can help the identification process, such as haplotype frequencies and Y-chromosome analysis.

When analyzing human skeletal remains, the goal of a medical examiner or a forensic anthropologist is to create a biological profile to help the narrowing down of potential identifications possible (Ballantyne et al. 2014; Kayser 2017; Kayser et al. 2004). A biological profile includes aspects such as possible age and biological sex. The most common practice is an analysis done by a forensic anthropologist using morphological traits to help estimate the potential sex and age of the individual. The biggest issue with doing this is that it is an educated estimate from the anthropologist's point of view that can differ from person to person. Since biological sex is one of the major categories used to identify remains, having a way to know if the individual is a biological male or female is essential (Butler and Li 2014; Ballantyne et al. 2014; Kayser 2017). The absence or presence of the Y-Chromosome is the primary way to distinguish biological sex, although not the only one. The biological sex of an individual is the sex that is determined by the absence or presence of the Y-chromosome in the 23rd set (Tseng 2008).

2.3.1 Biological Sex vs. Gender

There can be confusion when terms such as sex and gender are used. Both are used in forensic anthropology, but there is a major distinction between them and what they are used for. Biological sex refers to the differentiation of males and females on a biological and genetic level (Tseng 2008). The distinction comes from the absents or presence of the Y-chromosome in the 23rd set of chromosomes. Excluding rare circumstances, each parent passes either an X or a Y-chromosome down to their offspring. Mothers will always pass down an X, while fathers could

pass down either an X or a Y. The combination created determines the sex organs that typically develop in the offspring. Two X's will indicate that the individual is likely biologically female, while XY will likely indicate biological male (Tseng 2008). It is only “likely” however, as there are many additional genetic factors that play into biological sex and its outward expression. The biological distinction does not always reflect the individual in life. This is where the term gender is introduced.

Gender refers to the self-perception of oneself (Tseng 2008). Gender is an entirely socially constructed concept. It has played an active role in society throughout history, and education on the subject is growing exponentially. Individuals have the right to identify as anything they want, even when it does not conform to their biological sex. Skeletal remains and DNA can not inform a forensic anthropologist of an individual's gender. As a socially constructed concept, the biology that creates the differentiation of male and female doesn't necessarily influence gender. While the biological sex of an individual does not and cannot determine the gender of an individual, the knowledge of biological sex is an essential factor in identification (Kayser et al. 2004; Butler and Li 2014). Due to the growing acceptance of non-cis-gendered (cis denotes a person who identifies with their biological sex), that information is now more commonly known to investigators. This means that if the reported biological sex of an individual is known, the individual's biological profile can be compared to both cisgendered individuals and non-cisgendered who are biologically the same sex.

2.3.2 Biological Sex Identification

A DNA test that looks specifically for the presents of a Y-chromosome can indicate the biological sex (Kayser et al. 2004; Andersen and Balding 2017; Parsons et al. 2019). This method can also be helpful in a place where funds for testing are low. Many crime labs are

government-funded and are limited in the number of tests they can afford to run. A CODIS STR kit that can run approximately 200 samples costs over $5000 and is not always possible (“PowerPlex® 21 System” n.d.). While a Y-chromosome analysis doesn't give you universally usable results, it can provide a starting point for identification. A test that could do this is quantitative polymerase chain reaction or qPCR (Siljic et al. 2017; Hedman et al. 2011; Kayser et al. 2004; Ballantyne et al. 2014). This test uses a laser and fluorescent dye to quantify the amount of DNA in a sample as it is being amplified (replicated). In using it for biological sex determination, the Y-chromosome would be targeted. If the sample is amplified, it would indicate that the Y-chromosome DNA is present. This would then indicate that the individual is biologically male. A kit for this type of analysis costs a fifth of the price of a complete STR kit.

2.3.3 Current Application

While using DNA to identify an individual or their biological sex is being used today, a proper method to collect this DNA from skeletal remains is missing. Since its introduction, DNA has been researched endlessly, but bone-specific research comes up short. Hundreds of articles have been published about the research of DNA extracted from bone, but even in published articles, there is no official or universal way in which the bone samples are collected (Kayser 2017; Roewer 2019; 2013; Stray and Shewale 2010; Klavens et al. 2020; Shewale and Liu 2013). This is especially true for modern human remains. Y-chromosome and Y-STR studies are even more challenging to find. Articles using the Y-chromosome rarely use bone samples, and the ones that do are primarily in archaeological context (Ambers et al. 2018; Luptáková et al. 2011; Wang et al. 2021). Ambers et al. used a series of kits from different manufacturers to look at degradation between remains that had died at differing times, but all the samples used were pre-Civil War. While the data provided gives good insight and introduces some methods, they are

not always applicable to modern cases. Bones found in ancient and historic contexts typically have a different biological makeup. This is due to the breakdown of organic compounds in the bone over time (Ambers et al. 2018). The longer the individual has been dead, the less organic material is left; therefore, less DNA is available.

The major problem when needing to take DNA from skeletal remains is knowing where to take it. There is currently very little to no research on where it is best to take bone samples for DNA testing. The key to a successful test is having viable DNA and the research on where to find it has not been done (Klavens et al. 2020; Parsons et al. 2019; Kayser 2017; D'Amato, Benjeddou, and Davison 2009). Most of the published articles regarding bone DNA sampling take a sample from whatever bone is present and uses what they have. The biggest issue with having no method behind this is that every bone goes through different stages of degradation due to size and environment (Ambers et al. 2018; Andronowski et al. 2017).

Bones at a basic level are made up of collagen, an organic material, and hydroxyapatite, an inorganic material (White 2011). After death, the collagen will begin to break down, leaving the hydroxyapatite behind. This is why older bones are more fragile and harder to extract DNA from. Bones are also made up of different bone types that differ in structure and molecular properties. The outside layer of bone is called cortical bone (White 2011). The structure of this bone is very compact and gives the bone the rigid stability it needs. The inner layer of bone is the trabecular bone, which is called spongy bone in many cases due to its sponge-like texture. The trabecular bone is the location of red marrow, which forms blood cells (White 2011). While made of the same materials, cortical and trabecular bone degrade in different ways due to their structural makeup. Bones are exposed to many different environmental factors that affect how a bone degrades. For example, sun exposure for extended periods of time bleaches the bones white

and can cause them to crack. The exposure could affect the outside of the bone but not the inside. This could mean the cortical bone is too degraded for DNA testing while the trabecular is not (Emery et al. 2020; Stray and Shewale 2010). The different structures also mean that the bone cells are affected differently.

The differences in these details could be the reason for successful or failed testing. Knowing where the bones yield the best autosomal and Y-chromosome DNA is crucial to preventing failed testing. Failed tests are detrimental to crime labs, DNA labs, and organizations like the International Commission on Missing Persons (ICMP) who, are low on funds and time (Parsons et al. 2019; Kayser 2017; Roewer 2019; 2013). Knowing exactly where they need to drill, or at least an idea of where, can reduce time and money spent on each case and help combat the backlogs of testing still needing to be done. There is currently no research that differentiates cortical bone samples from trabecular ones in terms of DNA extraction yield. Most DNA sampling tends to use a mixed sample, but as mentioned above, different factors affect each bone type (Parsons et al. 2019; Kayser 2017; Roewer 2019; 2013). If each bone type degrades a different way, that means one of them should have better success in testing the DNA and knowing where to drill. Knowing what type of bone is needed is also information that is not known.

Another problem seen across all research regarding DNA sampling of bone is the amount of bone needed to run each test. Every published article tends to have no real idea of how much bone is required, where to get the sample, and how to get it (Kayser 2017; Roewer 2019; 2013; Stray and Shewale 2010; Klavens et al. 2020; Shewale and Liu 2013). All DNA extraction kits call for a specified weight of bone needed to utilize the kit effectively but do not inform users how to get it. Due to the lack of method-specific research, most analysts collect too much bone

material, such as Klavens et al., in their research on comparing DNA yield based on locations samples on the lower long bones (2020). They collected a range of 130-160mg of bone when accurate testing can be achieved with less than 10mg (Klavens et al. 2020). The cutting of large pieces of bone leaves apparent damage. While in a lab where the remains were donated for research, this is more acceptable; that is not always the case in a forensic context. The less obvious the sampling, the better it is, and a method to show this is needed in the field.

3.0 Methods

To test my hypothesis, equal numbers of cortical and trabecular bone samples were analyzed using quantitative polymerase chain reaction (qPCR). qPCR is used to determine the quantity of DNA molecules present in a given sample. To use qPCR for this project, samples were taken from human bone before going through a DNA extraction process and then be amplified in a qPCR machine.

The remains used to conduct this project were obtained from the Montana State Crime Lab located in Missoula, Montana. Initially, the individual was an unknown male found deceased in the Clark Fork River by some boaters in Missoula. The remains were sent to the crime lab, where a complete autopsy was performed. After the autopsy, the remains were professionally macerated by the crime using an enzyme-based solution of bleach and water at sub-boiling temperatures. Upon completing full skeletonization, the remains were then donated to the University of Montana Forensic Anthropology Laboratory (UMFAL) with a signed letter of donation from the Missoula County Deputy Coroner and the Missoula County Medical Examiner. Since the donation, the remains have been stored in the UMFAL with limited access limited to faculty and select graduate students.

While the remains were donated to the university, efforts to find the individual's identity continued. During the autopsy, tissue samples were taken for identification purposes and the DNA profile was put into CODIS. In May of 2021, the remains were identified as those of David James Smith. Analyses were placed on hold temporarily so permission from the next of kin could be obtained to continue the project. After locating the next of kin, they gave full permission for Mr. Smith's remains to stay in possession of the University of Montana Forensic Anthropology Laboratory for further analyses and educational purposes.

3.1 Sample Collection

A total of 80 samples were collected from across the remains (Table 4). Of the total, 39 are cortical bone, 39 are trabecular bone, and two are from the petrous portion of the right and left temporal bones. The petrous samples were used as comparison due to being the most commonly used for identification purposes due to their known high preservation rate (Gaudio et al. 2019). Samples were taken from the left side, right side, and the midline of the remains. The exact sampling location on each bone was determined by Keith Biddle M.A.

For DNA extraction and testing to be successful, the bone sample must be collected in a particular way. The finer the bone powder collected, the more successful the extraction. Due to the need to break down the bone during extraction to release the DNA from within the use of finely ground bone powder creates less work for the demineralization buffer in the extraction process. The finer powder will allow more DNA to be extracted because it gives the demineralization buffer a head start on the process. The less work the demineralization buffer must do, the more likely the DNA would be extracted.

3.1.1 Collection Process

Sample collection was conducted in the anthropology department's assigned drilling room. Before each use, all countertops, fume hoods, and equipment in the room were cleaned with a 50/50 solution of household bleach and tap water or DNA AWAY™. All individuals put on gloves, arm guards, masks, and safety glasses upon entering the room. All tools used were wiped down with DNA AWAY™. All other supplies including plastic ware, such as 1.5ml collection tubes and weigh boats, as well as metal instruments including the drill bits, were pre-sterilized using a Spectronics Corporation SPECTROLINKER™ XL-1500 UV Crosslinker

and/or a Mini High Temperature Sterilizer NV-210 autoclave machine for a minimum of 15 minutes, to eliminate possible contamination from prior uses and handling.

Before sampling, the bones were cleaned to remove possible surface contamination from any previous handling. The bones were soaked in a 3.5% solution of bleach and water for 15 minutes, followed by two rinses in distilled water. The bones were then left on UVed paper towels on the counter in the sterilized drilling room overnight to airdry fully. Bones were cleaned the day before they were drilled to maintain minimal contamination between cleaning and drilling.

The bone drilling samples were collected using a Dremel® with a 1mm dental burr drilling bit (Microcopy Dental, HP8). This is the best tool for this process as it not only causes minimal destruction but also grinds the bone into a very fine powder needed for extraction. Cortical bone samples were collected first by running the drill over the top surface of the bone at the pre-determined location. The drill was held perpendicular to the bone and was slowly moved in a linear pattern along the surface, making sure to remain on the surface only. The samples were collected in a sterilized weigh boat then transferred into a sterile, UV exposed (15 minute minimum), and labeled 1.5ml collection tube. The tubes containing the powdered bone sample were then weighed by being placed on a US Solid scale in grams that was zeroed out to the weight of an empty tube on the scale. The sample was then placed upside down with the bone powder collected on the closed lid of the collection tube it was in. The goal mass of each sample was approximately 0.08g-0.10g of powder to have enough for the extraction process. The final mass of the sample was then recorded. Trabecular bone samples were collected from the same locations as the cortical bone. The Dremel® was used to punch a small hole through the cortical

layer to reach the inner trabecular bone. The collection process then followed the same process as the cortical bone sampling.

After each sample was collected, the drill bit and the surface of the drilling area were wiped down with DNA AWAY™ to remove any DNA from the previous sample, and new plastic ware and gloves were used for the following collection. A new drill bit and gloves were used to prevent contamination between samples between each bone. After collections were completed for the day, all samples were placed in a refrigerator 13° to preserve the DNA. Drill bits and other metal tools were cleaned with DNA AWAY™ before being placed in the Mini High Temperature Sterilizer NV-210 autoclave for 60 minutes, then into the crosslinking machine for a minimum of 15 minutes. All surfaces were wiped down with a 50/50 solution of bleach and water or DNA AWAY™, and a UV light was turned on for approximately 30-60 minutes to aid in decontaminating the room.

3.2 DNA Extraction

A chemical reaction using bone lysates and demineralization buffer must happen to extract the DNA from the collected bone samples. These chemicals are designed to break down the inorganic calcium in the bones. Breaking down the calcium will release the DNA molecules from the within calcium matrix of the bone. After releasing the DNA from the bone powder, the DNA must be purified to ensure the sample is of good quality for analysis. The purification process is designed to isolate the DNA molecules from any other materials that may have ended up in the sample. Substances such as minerals or other substrates found in the bone may interfere with downstream analyses and must be removed.

Promega's Purification of DNA from Bone Samples Using Bone DNA Extraction Kit, Custom and DNA IQ™ Chemistry kit was used for this project. The protocol associated with this kit was also used but with modifications based on consultation with the representatives from Promega. These modifications included the mass needed from each sample, the machine used in the incubation process, and the time the samples needed to incubate based on the different machine. The modifications made were based on the availability of machines and the results of preliminary testing.

3.2.1 Extraction Process

In the sterilized drilling room, samples were removed from the refrigerator, and approximately 0.05g-0.1g of the bone powder were transferred to UVed 1.5ml LoBind collection tubes (Table 4). LoBind tubes are used in the extraction process because non-LoBind tubes allow the DNA sample to bind to the plastic coating inside the tube and cause the sample to be lost ("LoBind Protein or Genomic Microcentrifuge Tubes, Eppendorf®" n.d.). LoBind tubes are designed to minimize the amount of sample that binds to the tubes to maximize the sample. Once transferred to the new tubes, the samples are re-weighed, and the new mass is recorded. Samples are then moved to the Modern DNA Laboratory.

Before extraction began, the laboratory was sanitized with a 50/50 solution of bleach and water. All surfaces and instruments were sanitized with the bleach solution or DNA AWAY™. Gloves and masks were used to prevent contamination during the extraction process.

The first step done in the extraction process was to create the two bone lysis cocktails needed at different protocol steps. Each extraction done contained eight samples and an extract control; therefore, the reagent volumes were multiplied by 10 in order to have enough for the

extraction plus one to reduce possible pipetting errors. Lysis Cocktail A contains 4000µl of Demineralization Buffer, 400µl of Proteinase K, and 100µl of 1-Thioglycerol. Lysis Cocktail B contains 9900µl of Lysis Buffer and 100µl of 1-Thioglycerol. Also, at this time, 18 1.5ml LoBind collection tubes for future steps of the protocol were prepped by removing them from the Spectronics Corporation SPECTROLINKER™ XL-1500 UV Crosslinker and labeling each tube with the appropriate sample name. Each sample needs an additional two Lo-Bind tubes, one for DNA purification and one to hold the final eluted DNA sample.

After preparing the lysis cocktails, 400µl of Lysis Cocktail A was added to each sample and the empty extract control tube using a pipette with a sterile filtered tip. Each sample was then vortexed for approximately 10 seconds to mix. The samples were then placed in the Benchmark® Roto-Therm Mini Plus, preheated to 56ºC. Samples were left in the machine at a constant temperature of 56ºC for 30 minutes; samples were removed after 15 minutes and individually vortexed for approximately 5-10 seconds. At the end of the 30 minutes, samples were removed from the Roto-Therm and vortexed again for approximately 10 seconds to mix. Samples were then centrifuged in the Fisher Scientific accuSpin™ 400 for 5 minutes at 13,000xg.

Once removed from the centrifuge, the supernatant containing the extracted DNA was transferred into a pre-prepped, 1.5ml collection tube using a pipette with sterile filtered tips leaving the pellet of bone powder behind. The bone pellets were then discarded. In the tubes containing the supernatant, 800µl of Lysis Cocktail B was added to each sample and vortexed for approximately 10 seconds to mix.

3.2.2 DNA Purification

Since the DNA had been removed from the bone, it had to be purified to eliminate any possible impurities in the sample. The first step to purify the sample was to vortex the DNA IQ™ Resin to resuspend the magnetic beads into the resin. Using a pipette, 15µl of resin was added to each tube containing the unpurified DNA and vortexed for 3-5 seconds to mix. The samples were left to incubate at room temperature for 5 minutes and vortexed every 2 minutes. The resin contains magnetic beads that the DNA adheres to be washed and purified.

At the end of the 5-minute incubation time, the samples were vortexed again for 3-5 seconds then placed on a magnetic stand. The magnetic beads were allowed to pellet to the side of the tube. The lysate in the tube was then carefully removed from the tube and discarded using a pipette without disturbing the bead pellet. After the lysate was entirely removed, 100µl of Lysis Buffer B was added to each sample, vortexed for 3-5 seconds, and then placed back onto the magnetic stand. Once the beads were allowed to pellet to the side of the tube, the lysis buffer was carefully removed and discarded.

To further purify the DNA, 100µl of 1X Wash Buffer was added to each tube. The 1X Wash Buffer contained a 2:1:1 ratio of 2X Wash Buffer included in the DNA IQ™ kit, Isopropyl Alcohol, and 95-100% Ethanol. The samples were then vortexed for 3-5 seconds and returned to the magnetic stand. The wash buffer was removed and discarded once the beads were pelleted to the side of the tubes. The wash was repeated two more times for a total of three washes. After the last wash buffer was removed, the lids of the tubes were left open to allow all remaining wash buffer to evaporate and for the magnetic pellets to air dry for 5 minutes.

The last extraction step involves removing the DNA from the magnetic beads. After the 5-minute drying time, 50µl of Elution Buffer was added to each tube. The lids were closed, and the samples were vortexed for 3-5 seconds to resuspend the beads into the buffer. The samples were placed in a preheated Fisher Scientific Isotemp® at 65ºC and allowed to incubate while stationary for 5 minutes. At the end of the 5 minutes, the samples were removed from the heater and vortexed for 3-5 seconds before being placed back on the magnetic stand. When the magnetic beads were pelleted, the eluted DNA was transferred to the final pre-prepped 1.5ml LoBind tube. The completed samples were stored in a refrigerator at 4ºC until needed for qPCR analyses.

3.2.3 Qubit ™ Analysis

When the extraction of each sample was complete the Qubit™ dsDNA HS Assay was used to read a preliminary concentration of DNA in each sample. The Qubit helps by showing what samples may have not been extracted correctly or if there is any contamination in each extraction control.

For each extraction, 11 sterilized 0.5mL PCR tubes compatible with the Qubit ™ Fluorometer model 4 were labeled for each sample and for standards #1 and #2. For the standards, 190µl of the Qubit™ working solution was added to each tube followed by 10µl of the appropriate standard. Next 198µl of the working solution was added to the remaining tubes followed 2µl of the eluted DNA, including the extract control. Each tube was vortexed for 5-10 seconds and left to incubate at room temperature for approximately two minutes. After incubation the tubes were wiped down to ensure the outside of the tube had nothing on it that could interfere with the readings. Once cleaned, the standards were placed into the Qubit ™

Fluorometer one at a time. Once the standards had been read, each sample was run through the machine one at a time and the results were recorded (Table 4).

3.3 qPCR

Quantitative Polymerase Chain Reaction (qPCR) is a reaction to quantify the amount of DNA molecules present in each sample (Kralik and Ricchi 2017). The samples are amplified by the qPCR machine while simultaneously accumulating molecules of florescent chemicals designed to target specific parts of the DNA, and the more of the target, the brighter the fluorescence. The machine then reads the fluorescent markers to quantify the amount of DNA in each sample, in comparison to known standards. For this project, the Plexor® HY System for the Stratagene Mx3000P® and Mx3005P™ Quantitative PCR Systems kit produced by Promega was used along with its accompanying protocol.

This kit was created to quantify both human autosomal DNA and human Y-chromosome DNA. In this kit, four different fluorescent dyes are added to each sample, allowing the qPCR machine to read the amount of autosomal and Y-chromosome DNA present and an Internal PCR Control (IPC) and passive reference. The fluorescein (FAM™) dye targets and detects a 99bp section of chromosome 17. The data this dye produces indicates the total amount of autosomal DNA in each sample. The CAL Fluor® Orange 560 dye targets and detects a 133bp section of the Y-chromosome and indicates the total Y-chromosome DNA in the samples. CAL Fluor® Red 610 dye is added to the reaction to monitor any inhibition of amplification in the samples.

The last dye, IC5, is a reagent used as a passive reference and is not involved in the qPCR. It is used to normalize the differences between wells that may occur in fluorescence signal of the other dyes (Jordan and Kurtz 2010). These differences can occur due to pipetting

errors that cause less of the master mix containing the dyes to be added. If one sample was to have less master mix, and therefore less of each dye, the sample may not fluoresce as bright as other samples even if it were to have the same amount of DNA (Jordan and Kurtz 2010). The IC5 dye will constantly fluoresce in the sample. This constancy relative to the other reporting dye signals creates a reference to base the florescence on, and therefore the sample with the less master mix would be reduced in terms of its relative fluorescent readings (Jordan and Kurtz 2010).

The Plexor™ technology in this kit uses an interaction between two novel bases created by Promega (Hooper 2007). In one primer included in the kit, the bases, isoguanine (iso-G) and 5'-methylisocytosine (iso-C), are added to the DNA strands during amplification and only pair with each other. In the reaction, one of the PCR primers is synthesized with the fluorescent dye and the iso-C at the 5'-end. Also included in the reaction mix is dabcyl-iso-dGTP. These nucleotides are incorporated into the DNA strands during amplification at the 3'-end, complementary to the iso-C on the 5'-end (Hooper 2007). The dabcyl-iso-dGTP acts as a fluorescent quencher and will quench the fluorescent dye attached at the 5'-end when the annealing and extension step of the qPCR is complete (Hooper 2007).

3.3.1 qPCR Setup

The qPCR template preparation was conducted in the University of Montana Modern DNA Laboratory. Before the qPCR setup began, the laboratory was sanitized with a 50/50 solution of bleach and water. All surfaces and instruments were wiped down with the bleach solution or DNA AWAY™. Gloves and masks were used to prevent contamination during the setup process.

As per manufacturer's instructions, the kit was kept at 2-10°C for long-term storage. The reaction setup started by thawing the Plexor® HY 2X Master Mix, Plexor® HY 20X Primer/IPC Mix, and amplification grade water at room temperature. After fully thawed, the Plexor® HY 2X Master Mix and Plexor® HY 20X Primer/IPC Mix were vortexed for 10 seconds to mix. The reaction mix was prepared by combining 10µl of Plexor® HY 2X Master Mix, 7µl of amplification grade water, and 1µl of Plexor® HY 20X Primer/IPC Mix per number of reactions plus 2 in a sterilized 2ml tube. For this project, 96 reactions were run simultaneously, so the reaction mix was prepared for 98 reactions. Extra mix ensures enough mix for each reaction while reducing possible pipetting errors. The mixture was then vortexed for approximately 10 seconds to mix. The mixture was then poured into a reagent reservoir that allows the use of an 8-tip-pipette.

Using an 8-chanel pipette, 18µl of the reaction mix was put into each well of a sterilized 96-well optical-grade qPCR plate. The reaction mix was placed in every well, including the standards and no-template controls (NTC). Each sample, standard, and NTC were run twice, and the results were averaged to reduce variability.

For the NTC, located in cells H1 and H2, 2µl of the TE^{-4} buffer was added to the reaction mix in place of DNA. TE^{-4} buffer was made using 1000µl of Tris HCL, 20µl of EDTA, and 9900µl of amplification grade water. The NTCs act to detect any contamination in a qPCR run and should have no DNA amplification. The DNA samples containing an unknown amount of DNA were located in columns 3-12. Each well intended for the unknown samples had 2µl of DNA added to each as indicated in Tables 1 and 2.

Table 1: qPCR Plate 1 Setup

STD 50ng/µl	STD 50ng/µl	LC3	LC3	FEM3	FEM3	LH1	LH1	LMC3A	LMC3A	LOS5	LOS5
STD 10ng/µl	STD 10ng/µl	LC4	LC4	FEM5	FEM5	LH2	LH2	LMC3B	LMC3B	LOS6	LOS6
STD 2ng/µl	STD 2ng/µl	CL3	CL3	FEM6	FEM6	LH3	LH3	MC3A	MC3A	OS5	OS5
STD 0.4g/µl	STD 0.4g/µl	CL4	CL4	FEM7	FEM7	LH5	LH5	MC3B	MC3B	OS6	OS6
STD 0.08ng/µl	STD 0.08ng/µl	LFEM3	LFEM3	LFIB1	LFIB1	HUM1	HUM1	LMT2A	LMT2A	LRAD1	LRAD1
STD 0.016ng/µl	STD 0.016ng/µl	LFEM5	LFEM5	LFIB2	LFIB2	HUM2	HUM2	LMT2B	LMT2B	LRAD2	LRAD2
STD 0.0032ng/µl	STD 0.0032ng/µl	LFEM6	LFEM6	FIB1	FIB1	HUM3	HUM3	MT3A	MT3A	LRAD3	LRAD3
TE^{-4}	TE^{-4}	LFEM7	LFEM7	FIB2	FIB2	HUM5	HUM5	MT3B	MT3B	LRAD5	LRAD5

Table 2: qPCR Plate 2 Setup

STD 50ng/µl	STD 50ng/µl	RAD1	RAD1	LSC1	LSC1	TIB1	TIB1	U1	U1	LV2A	LV2A
STD 10ng/µl	STD 10ng/µl	RAD2	RAD2	LSC2	LSC2	TIB2	TIB2	U2	U2	LV2B	LV2B
STD 2ng/µl	STD 2ng/µl	RAD3	RAD3	GF1	GF1	TIB3	TIB3	U3	U3	T2A	T2A
STD 0.4g/µl	STD 0.4g/µl	RAD5	RAD5	GF2	GF2	TIB5	TIB5	U5	U5	T2B	T2B
STD 0.08ng/µl	STD 0.08ng/µl	LR1A	LR1A	LTIB1	LTIB1	LU1	LU1	LP	LP	SAC1	SAC1
STD 0.016ng/µl	STD 0.016ng/µl	LR1B	LR1B	LTIB2	LTIB2	LU2	LU2	RP	RP	SAC2	SAC2
STD 0.0032ng/µl	STD 0.0032ng/µl	R1A	R1A	LTIB3	LTIB3	LU3	LU3	C2A	C2A	STE3	STE3
TE^{-4}	TE^{-4}	R1B	R1B	LTIB5	LTIB5	LU5	LU5	C2B	C2B	STE4	STE4

The last step for the setup was to create serial dilutions of the Plexor® HY Genomic DNA Standard to create a reference ladder during the reaction. A reference ladder is used during qPCR to give the machine known DNA amounts to compare the unknown samples to. The male DNA standard is analyzed in the same way as the other samples and the amount of fluorescence is read. Because the standards contain known amounts of DNA, a comparison can be made to quantify the amount of DNA in the unknown samples. To prevent contamination to the unknown and NTC samples, the highly concentrated DNA standards were handled last. Before the first use, the DNA standard was moved to a refrigerator set at 4°C overnight. To begin the standard dilutions, the Plexor® HY Male Genomic DNA Standard, 50ng/µl, was thawed and vortexed for approximately 10 seconds.

For the dilutions, 10µl of undiluted 50ng/µl standard was added to the first tube of a sterilized 0.2ml 8-strip followed by 40µl of the TE^{-4} buffer sing a sterilized pipette. The mixture was then vortexed for approximately 10 seconds, creating a 10ng/µl dilution. After being vortexed, 10µl of the 10ng/µl dilution was added to the second tube, followed by 40µl of the TE^{-4} buffer. The mixture was vortexed for approximately 10 seconds, creating a 2ng/µl dilution. This process was repeated creating 0.4ng/µl, 0.08ng/µl, 0.016ng/µl, and 0.0032ng/µl dilutions (Table 3). After handling the highly concentrated DNA standards, new gloves were put on to avoid cross-contamination.

Table 3: Concentrations of the DNA standard for the serial dilutions.

Concentration	Volume of DNA	Volume of TE–4 Buffer
50 ng/µl	Use undiluted DNA	0µl
10 ng/µl	10µl of undiluted DNA	40µl
2 ng/µl	10µl of 10ng/µl dilution	40µl
0.4 ng/µl	10µl of 2ng/µl dilution	40µl
0.08 ng/µl	10µl of 0.4ng/µl dilution	40µl
0.016 ng/µl	10µl of 0.08ng/µl dilution	40µl
0.0032 ng/µl	10µl of 0.016ng/µl dilution	40µl

The plate was then sealed with manufacturer-approved optical caps. If the incorrect cap or plate were used, the qPCR machine would not be able to read the fluorescent labels in the samples. The sealed plate was then centrifuged briefly to ensure the contents of each well were at the bottom.

3.3.2 Thermal Cycling

The sealed plate was taken to the University of Montana Genomics Core Laboratory for analysis. The Stratagene Mc3000P® was used for this project. After arriving at the Genomics Core, the machine was set up per the manufacturer's instructions. The plate was then placed into the machine to go through the thermal cycling process. The thermal cycling program consisted of 87 cycles allowing for amplification and reading of the fluorescent markers.

The first step in the thermal cycling was the initial denaturation at 96ºC for two minutes. This step activates the reaction mix to begin the denaturation, which melts open and separates the two strands of DNA into two single-stranded DNA templates. Initial denaturation was completed for one cycle only.

The next step was the denaturation of the sample at 95ºC for 5 seconds. This step continues what the first step does by melting open the DNA strands. Next was the annealing and extension step at 60º for 40 seconds immediately following the denaturation. During annealing, DNA primers from the reaction mix attach to the appropriate ends of the targeted sequences in the sample. DNA polymerase then attaches to the primed template and begins to add complementary nucleotides to the single strand of DNA. The extension step extends the DNA polymerase completing the other side of the single-strand DNA producing a replicate of the original double-stranded DNA of the sample.

While in the annealing and extension step of the cycle, the four fluorescent dyes and dabcly-iso-dGTP were incorporated into their targeted sequences, allowing the machine to read how much each color fluoresces. When the DNA is double-stranded, the dabcly-iso-dGTP and iso-C are together they quench the fluorescent signals, which the machine reads as the amplification process continues, the number of signals decreases. When the strands go back through the denaturation step and the strands separate the increase of the fluorescent signal. The denaturation and annealing, and extension steps were repeated for 38 cycles.

The last step was the melt temperature curve. This step started at an initial temperature of 65ºC and increased by 0.6ºC each cycle, holding for 40 seconds each cycle. The melt curve step was repeated for 48 cycles. During this step, the melting temperature of the amplification products were determined. This data was what identified the different sequences being analyzed in the samples. The melting cycle was designed to identify the different amplicons for autosomal DNA sequences and Y-chromosome sequences for this kit and project. This process was repeated for plate 2, which contained the other half of the samples.

3.4 Analysis

Once the samples had completed the thermal cycling, the data collected by the Stratagene Mc3000P® was imported to the Plexor® Analysis Software to analyze the results from the qPCR. The data was automatically graphed, and a standard curve and expected melt threshold for each dye had to be added to allow for proper reading of the raw data. The standard curves showed a 99.55% efficiency for plate one and a 99.30% for plate 2. The melt thresholds for each dye fell within the correct range, indicating that the standards were read correctly. Once complete, the normalized raw data was exported into Microsoft® Excel® for statistical analysis.

In Microsoft® Excel®, the data from each plate were combined and organized. Due to the duplication of each sample for the qPCR, each sample had two separate molecular yields for both autosomal and Y-chromosome DNA. The two yields of each type were averaged together to create one yield for autosomal DNA and one yield of Y-chromosome DNA for each sample. Basic statistical analyses for averages were run on the samples to determine what bone type yielded higher amounts of Y-chromosome DNA and autosomal DNA. Other factors such as pre-extraction powder weight, Qubit™ results, siding, and bone condition were also looked at to see could have influenced the results.

4.0 Results

4.1 Y-Chromosome DNA Yield

All samples except for seven yielded a readable amount of Y-Chromosome DNA. All four NTCs had no reads, indicating no contamination. The samples from LRAD1 and STE4 did not have reads due to circumstances unrelated to the qPCR. LRAD1, the cortical bone sample for the left radial head, did not amplify due to a defect in the final collection tube the sample was stored in after extraction. STE4, the trabecular sample from the distal sternal body, was not run because the qPCR master reagent ran out during plate setup. The last sample that did not provide a Y-chromosome DNA yield was FEM7, the trabecular sample from the right femoral intercondylar fossa, this sample did not contain a readable amount of Y-chromosome DNA and a zero was used for analysis purposes.

The first analysis was conducted using the AUTOSUM function in Excel® to calculate and compare the average yield from both runs of the cortical bone samples against the trabecular bone samples. The average yield of Y-chromosome DNA in the cortical bone samples equaled 0.09890ng/µl. The trabecular bone samples were analyzed the same way. The trabecular bone samples, including both petrous portions of the temporals, had an average Y-Chromosome yield of 0.02130ng/µl of DNA (Table 4).

Table 4: Averages of Y-Chromosome and autosomal yield for each bone type.

Cortical vs. Trabecular Averages (ng/µl)		
Y	Cortical Average	0.09890
Y	Trabecular Average	0.02130
Auto	Cortical Average	0.28260
Auto	Trabecular Average	0.10484

The top ten highest yields and the bottom ten lowest DNA yields were compared (Table 5). Of the top ten, 90% were cortical bone, and the bottom ten were 90% trabecular bone. A T-Test was also run comparing the means of the cortical and trabecular bone samples (Table 6). The mean of the cortical bone samples was 0.10150ng/µl with a variance of 0.01820ng/µl, and the trabecular bone samples were 0.02209ng/µl with a variance of 0.00102ng/µl. The p-value calculated was <0.0, suggesting that the cortical and trabecular bone samples are statistically distinct.

Table 5: The top ten and bottom ten sample based on the Y-chromosome average.

Side	Bone	Location	Weight (g)	Sample Type	Y-Chromosome (ng/µl)	Autosomal (ng/µl)
Top 10 Samples Based on Average Y-Chromosome Yield						
Right	Femur	Inter Condylar Fossa	0.150	Cortical	0.59377	1.53072
Right	Tibia	Mid-Diaphysis	0.140	Cortical	0.43065	0.98559
Right	Tibia	Tibial Plateau	0.060	Cortical	0.33054	1.41029
Right	Femur	Nutrient Foramen	0.080	Cortical	0.30707	0.60443
Right	Clavicle	Lateral End	0.078	Cortical	0.27307	0.64781
Midline	C. Vertebrae	Body/Dens	0.100	Cortical	0.20719	0.65028
Right	Scapula	Glenoid Fossa	0.065	Cortical	0.18945	0.73983
Midline	Lumbar Vertebrae	Body	0.112	Cortical	0.18860	0.54553
Left	Femur	Inter Condylar Fossa	0.096	Cortical	0.16343	0.47739
Left	Radius	Radial Tuberosity	0.113	Trabecular	0.14771	0.64271
Bottom 10 Samples Based on Average Y-Chromosome Yield						
Left	Rib	Rib 1	0.080	Trabecular	0.00341	0.04044
Left	Femur	Nutrient Foramen	0.062	Trabecular	0.00332	0.03646
Midline	Lumbar Vertebrae	Body	0.100	Trabecular	0.00283	0.01111
Right	Radius	Radial Tuberosity	0.072	Trabecular	0.00272	0.04302
Midline	T. Vertebrae	Body	0.068	Trabecular	0.00245	0.00552
Left	Fibula	Styloid Process	0.067	Trabecular	0.00168	0.00397
Midline	Sternum	Distal Corpus Sterni	0.067	Cortical	0.00133	0.00292
Left	Tibia	Tibial Plateau	0.106	Trabecular	0.00122	0.00380
Midline	Sacrum	Sacral Promontory	0.073	Trabecular	0.00034	0.00203
Right	Femur	Inter Condylar Fossa	0.130	Trabecular	0.00000	0.00337

Table 6: T-Test results for means of the Y-chromosome and autosomal DNA yield.

	Y-Chromosome	*Autosomal*
Mean	0.060	0.194
Variance	0.011	0.093
Observations	77	77
Pearson Correlation	0.933	
Hypothesized Mean Difference	0	
df	76.000	
t Stat	-5.589	
P(T<=t) one-tail	0.000000170	
t Critical one-tail	1.665	
P(T<=t) two-tail	0.000000341	
t Critical two-tail	1.992	

4.2 Autosomal DNA Yield

As a comparison, the averages for the autosomal DNA yield were also calculated. The same samples were averaged based on their bone type. The cortical bone samples averaged 0.28260ng/µl, and the trabecular bone samples averaged 0.10484ng/µl (Table 4). The top ten highest yields were 90% cortical bone, and the bottom ten lowest yields were 80% trabecular bone (Table 5). A T-Test analysis was run comparing the yields of the autosomal DNA and the Y-chromosome DNA. The Pearson Correlation coefficient was 0.933, a t-Stat of -5.589, and the p-value was <0.001.

4.3 Petrous Sample Comparison

The petrous portion of both the left and right temporal bone were run to compare the primarily used location to the post-cranial skeletal elements. The left petrous portion had a Y-chromosome yield of 0.00705ng/µl of DNA and an autosomal yield of 0.02772ng/µl (Table 7). The right side had a Y-chromosome yield of 0.00619ng/µl and an autosomal yield of

0.01469ng/µl of DNA. When put in descending order based on the Y-chromosome yield, the petrous portions rank number 52 and number 55 out of 80.

Table 7: Results from the petrous portions of the temporal bones.

Side	Bone	Location	Weight (g)	Sample Type	Y-chromosome (ng/µl)	Autosomal (ng/µl)
Left	Temporal	Petrous Portion	0.083	Trabecular	0.00705	0.02772
Right	Temporal	Petrous Portion	0.080	Trabecular	0.00619	0.01469

4.4 Other Factors Analyzed

Due to signs of overprocessing, the samples were broken down by side. Overall, the samples from the right side had an average of 0.08176ng/µl, the midline average was 0.10376ng/µl, and the left side average was 0.03754ng/µl. Of the top 10 highest yield amounts based on the Y-chromosome data, 60% were from the right side, 20% were from the midline, and 20% were from the left side.

The correlation between the DNA yield and the pre-extraction weight in grams was calculated to test the validation of using less bone powder to limit the destruction. For the Y-chromosome DNA yields, the correlation coefficient of each sample's yield and the pre-extraction weight were calculated to be 0.455. The autosomal yield correlation coefficient with the pre-extraction weight was 0.393. The distribution of the Y-chromosome molecular yield by weight is shown in Figure 1.

The correlation between the Qubit™ results and the DNA yields was also calculated. This was to test the value of using the Qubit™ before downstream analysis. For the Y-chromosome yield compared to the Qubit™ value, the correlation coefficient was 0.053. The correlation coefficient for the autosomal yield was 0.134 (Figure 2).

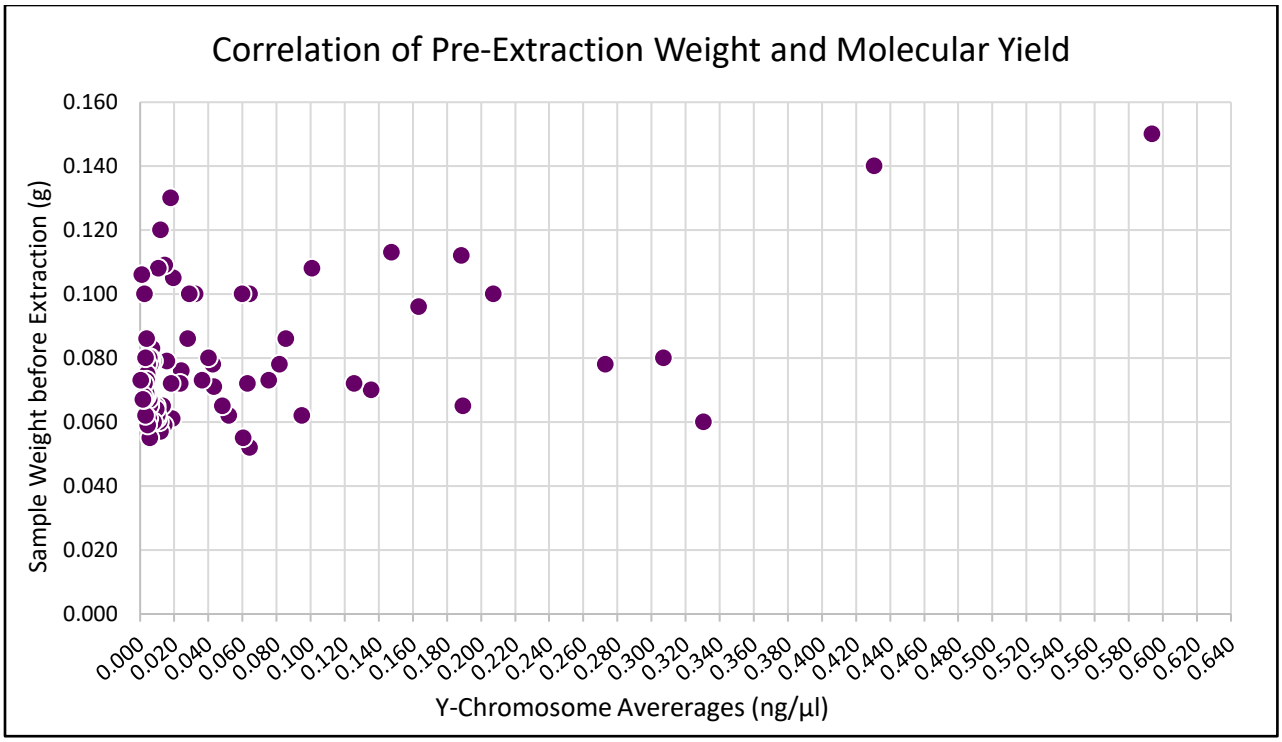

Figure 1: Distribution of samples when the pre-extraction weight and the average Y-chromosome yield were compared.

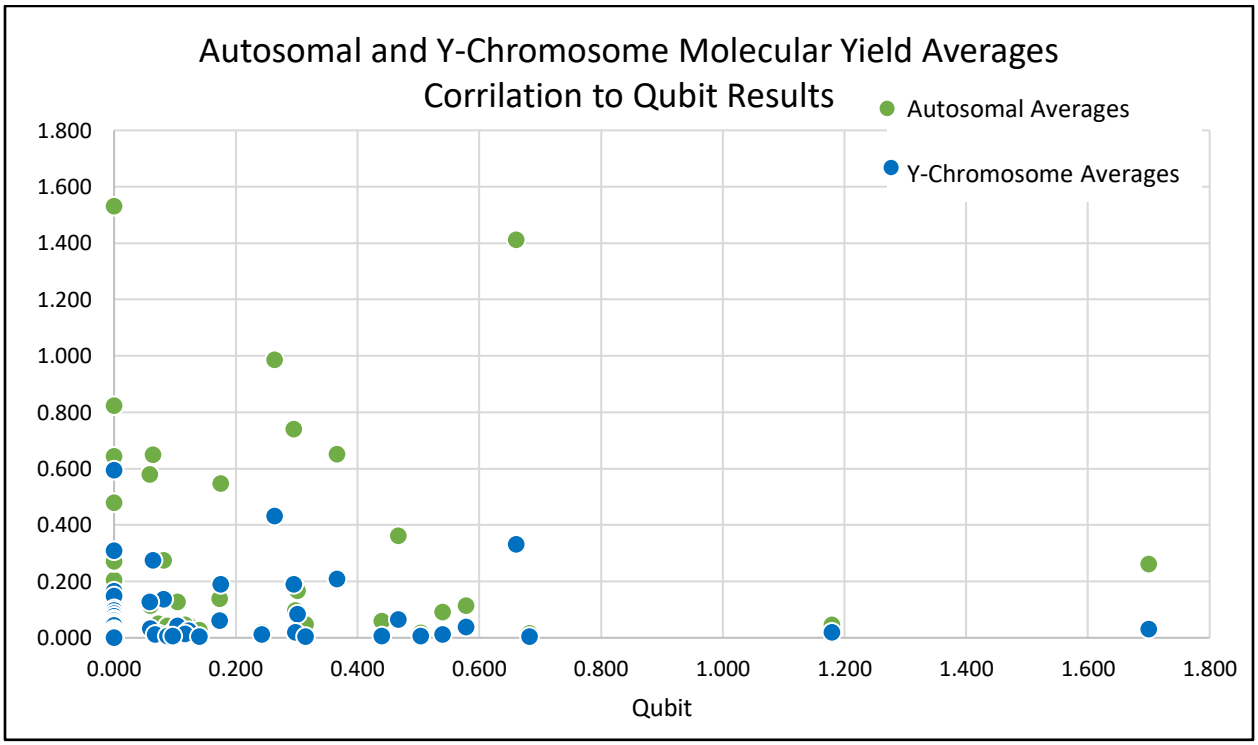

Figure 2: Distribution of samples based on the Qubit™ results and the actual recorded yield.

5.0 Discussion

5.1 Cortical Bone vs. Trabecular Bone

The main goal of this research project was to analyze the molecular yield of Y-chromosome DNA from samples of cortical bone and trabecular bone to determine what type is best for sampling. The research conducted was a preliminary experiment to provide data that could help improve sampling methods and analysis of DNA in modern human skeletal remains.

5.1.1 Hypothesis

The hypothesis stated that trabecular bone samples would yield higher amounts of Y-chromosome DNA than the cortical bone samples due to the structure. The sponge-like configuration provides increased surface area, allowing for more cellular activity. The location of the trabecular bone inside the bones would limit contamination from outside contaminates that the cortical bone is exposed to.

The hypothesis was not supported by the data gathered for this project. Overall, the cortical bone samples had higher DNA yields compared to the trabecular. When put into descending order based on the Y-chromosome yield, 75% of the samples in the top 20 were cortical bone. The trabecular bone samples are towards the bottom of the ranking and are from skeletal elements that showed a high yield for both samples. The higher yields from the cortical bone samples could be due to the bone structure combined with environmental factors observed such as exposure to the river and the post-mortem over-processing.

Cortical bone is comprised of the same materials as trabecular bone but is tightly woven to provide the rigid structure the bones need. The cortical bone has more cellular activity in life due to the stresses of proving the main structural integrity of the bone. With the cortical bone

being a tighter structure and subjected to more turnover during life, the bone cells and their associated DNA are most likely in a higher concentration than the trabecular bone.

5.1.2 Comparisons

In addition to looking at solely the Y-chromosome DNA yield for each bone type, the autosomal DNA yield was also analyzed. The comparison between these two provides more data on each bone type and allows for potential contamination to be seen. Like the Y-chromosome DNA, the autosomal yields showed that the cortical bone samples produced the higher yields. When compared to the Y-chromosome, the results were very similar.

Overall, the autosomal yields were significantly higher than those of the Y-chromosome. While the autosomal yields were higher, the samples that had higher autosomal yields consistently had higher Y-chromosome yields as well. The correlation coefficient of 0.933 and the p-value of 0 from the T-Test show that the samples are highly correlated. This result indicates that Y-chromosome DNA is consistently amplified in male samples. The close correlation also shows that there is minimal to no outside contamination. If the yields did not show a correlation between the two amplification loci, contamination could have occurred, causing the results to be skewed.

The petrous portion of the left and right temporal bones were also amplified during qPCR to compare them to the post-cranial skeletal elements. The known preservation rate of this element makes it ideal for sampling for identification purposes. If a skull is found with a set of skeletal remains, sampling tends only to be done from this location. In this project, the samples taken from the petrous portions did not yield the highest amounts of DNA for either autosomal or Y-chromosome as the other skeletal elements. Both samples were in the bottom half of the

samples based on the Y-chromosome DNA yields. This result was not expected as the petrous is more often used for DNA testing than post-cranial elements. This result could be attributed to environmental factors opposed but can not be proven without more research.

5.2 Limitations

This research had limitations that could have influenced the data collected and future research on DNA analysis in modern human bone. These limitations include damage due to post autopsy processing, limited sample size, and limited supplies and funding for the project. These limitations produced possible discrepancies in the data and need to be considered when using it for future projects.

5.2.1 Processing Damage

The primary influence that could have contributed to possible skewed results is the overall condition of the skeletal remains. A significant amount of soft tissue remained when the remains were recovered, and an autopsy was conducted. After the autopsy was completed, the remains were processed to remove the soft tissue using a standard method involving heat and an enzyme-bleach solution. This combination of the constant heat and the corrosive bleach caused some elements to become brittle and compromised for DNA analysis. Overexposure to the heat and bleach resulted in the breakdown of the bone and, therefore, the breakdown of the cells and their associated DNA.

Once the results were analyzed, the top ten and bottom ten elements based on the Y-chromosome yield were visually analyzed to assess their condition and the possible influence of processing damage on the results (Figures 3-4 and 13-15). The bone samples in the top ten came from bone that was in excellent condition. These bones were not brittle or appeared to be overly

bleached. The bone condition was different for the bone samples in the bottom ten. Overall, these bones had more variation in their condition. Most of the bones showed signs of processing damage. These bones tended to be very dry and appeared an unnatural shade of white compared to the top ten.

The bones most affected were trabecular samples located along the lower midline of the thorax. This indicates that the remains were most likely placed in the enzyme-bleach solution in a prone position. The elements located closer to the bottom of the processing vessel were exposed to higher heat than those further away. The breakdown of the bone potentially allowed the bleach solution to enter the inside of the bone and damage the cells inside. It is most likely that some of the results could be attributed to the damage produced by the post-mortem processing. This is further supported in the data from some of the samples collected from the bone that was in excellent condition. The trabecular bone samples that yielded the amounts on the higher end of the spectrum came from bone that did not have any visual damage or had thicker cortical bone surrounding it.

5.2.2 Sample size

The sample size of one used for this project was too limited for a conclusive result. The use of only one individual does not show an overall picture of bone type superiority in DNA testing. The skeletal remains were exposed to various post-mortem environmental factors that affected the viability of the DNA in each sample. The exposure to the Clark Fork River after death and the processing damages affected this individual, altering the overall bone condition. Due to these environmental aspects, the results are only limitedly informative on a larger scale.

The results obtained from the data could be strictly attributed to the condition of the remains and could have shown a different outcome under a different set of circumstances. More samples from multiple individuals from various post-mortem conditions would have increased the validity of the study and provided more conclusive results.

Figure 3: Photo of the right tibia showing the sample location for the mid-diaphysis. This location was the second best overall based on the Y-chromosome yield.

Figure 4: Photo of the left first rib. This bone was in the bottom ten and shows signs of overprocessing.

5.2.3 Limited Supplies

Limited supplies were a significant limitation for this project. Due to the cost of supplies, a limited number of samples could be analyzed for yield. Over 300 bone samples were collected from the remains, but only 80 could be used for this project. The Plexor® HY System for the Stratagene Mx3000P® and Mx3005P™ Quantitative PCR Systems kit used in this project only contained enough reagents to run approximately 200 reactions. This amount of reagent needed must include enough for the standards, NTCs, and unknown samples. Funding for this project was limited to $1000, and the kit was $991.

The initial sample size for this project had to be limited to 80 samples so there would be enough reagents for all samples to be run twice and the 36 standards and NTCs. The total number of reactions in the project was 192, not including the extra reagent to prevent pipetting errors. The kit did not contain enough reagents to run all the samples leading to the removal of one sample, and did not allow for any re-running of samples that had unexpected results, such as FEM7 and LRAD1.

5.3 Significance

While there were limitations to the project, the data did provide information that could be expanded upon with more research and an increased sample size. There was a notable difference in the yields of DNA based on bone type in this individual. Differences in DNA yield from the two bone types haven't been examined for modern remains. The data collected in this project could help improve the methods currently used in DNA sampling from human bone by introducing the idea that bone types preserve DNA differently.

5.3.1 Pre-Extraction Weight

The weight of each sample was also compared to the yield and provided important information in this project. When doing the extractions, the Plexor® HY System for the Stratagene Mx3000P® and Mx3005P™ Quantitative PCR Systems protocol instructed for 0.10g of bone powder to be used for each sample. To prevent extensive damage, limited amounts of powder were collected from each location on the remains. The kit was purchased after the drilling was completed, and some samples did not meet the 0.10g requirement. The larger than expected bone powder amount led to discussions with the manufacturer, who modified the protocol from using the 0.10g to using a range of 0.025g-0.08g. This change in protocol allowed for a variety in the weight of samples and prevented further damage to the remains.

After the samples were analyzed, the correlation between the pre-extraction weight and the average Y-chromosome DNA and autosomal DNA yield was calculated. This correlation analysis showed that there was weak to no correlation between the pre-extraction weight and the recorded final yields. The lack of correlation between the pre-extraction weight and the yield supports the idea that bone samples can be successfully collected and analyzed without significant damage. Samples from the lower side of the weight spectrum did just as well as some with the greater start weight and vis vera with the lower yield samples.

5.3.2 Qubit™ Results

The Qubit™ results are also significant to future research in molecular anthropology. When conducting this research, the data provided by Qubit™ was used as a tool to test the success of extraction and to see if the samples had contamination in the extraction process. Less than half of the samples in the data had a read from the Qubit™. Most of the samples indicated

that the amount of DNA detected was 'too low to read.' The cortical bone sample collected from the intercondylar fossa of the right femur had the highest yield of both Y-chromosome DNA and autosomal DNA, but Qubit™ had indicated that the DNA amount before extraction was 'too low to detect.

Like the pre-extraction weight, the Qubit™ result and the average yield of both the Y-chromosome DNA and the autosomal DNA for each sample were analyzed for their correlation. Both calculations indicate no correlation between the two measurements. The data shows that the concentration calculated by running the samples through Qubit™ does not necessarily indicate the calculated yield by qPCR. The inaccurate data could be a problem, especially when looking at the extract controls. If the Qubit™ is reading one of the best samples in the data set at 'too low to read,' could the 'too low to read' result in the extract control be inaccurate too? Further research on the accuracy and usefulness of Qubit™ needs to be done. Inaccurate testing uses up the limited amount of DNA extract that could be saved for a test that is proven to be more helpful.

5.4 Future Directions

The main idea behind this project was to create a better and less destructive method for identifying human remains through DNA analyses when traditional methods prove unsuccessful. The preliminary results produced by this project can lead to future projects on improving DNA sampling and extraction methods in human bone for identification purposes.

The number of unidentified deceased individuals worldwide is only growing, and the longer it takes, the less likely they will ever be identified. Something needs to be done to give

these individuals their names back. If the methods and accuracy of bone DNA analysis are improved, it could increase the number of identified individuals.

The next step in this research is to use the preliminary results from the different bone types and the locations tested to collect samples from unidentified remains that have not had successful DNA analysis. The samples, if extracted successfully, could then be used to create CODIS profiles or forensic genealogical profiles. Forensic genealogy is increasingly becoming a valuable source of potential identification when CODIS cannot provide any matching profiles.

6.0 Conclusion

The sampling of DNA from modern human bone still lacks methods that provide information on where and how to collect samples from the bone that will provide good results while also limiting the damage to the remains. While this project is a preliminary study on this topic, it provided important information that can be utilized and improved in future research. This project has shown that while most methods do not differentiate between bone types in samples, it could affect success in sampling.

The project also provided insight into other aspects of the sampling and DNA extraction processes that could affect what results are seen. Information regarding the post-mortem processing of the remains, the pre-extraction weight of the bone powder samples, and the accuracy of Qubit™ fluorometer readings was discovered in the process of testing the hypothesis. Together, this information could improve how remains are processed without causing damage, how the bone samples are collected for successful extraction and the accuracy of a well-used piece of technology in the lab.

Further research on this topic must be done to increase the validity of the results. Still, the preliminary data has provided a stepping stone in the right direction to improve how DNA sampling from modern human remains is done.

References

"2020 NCIC Missing Person and Unidentified Person Statistics." 2020. File. Federal Bureau of Investigation. 2020. https://www.fbi.gov/file-repository/2020-ncic-missing-person-and-unidentified-person-statistics.pdf/view.

Adams, Dwight. 2002. "The FBI's CODIS Program." FBI. May 14, 2002. https://www.fbi.gov/news/testimony/the-fbis-codis-program.

Ambers, Angie, Jitka Votrubova, Daniel Vanek, Antti Sajantila, and Bruce Budowle. 2018. "Improved Y-STR Typing for Disaster Victim Identification, Missing Persons Investigations, and Historical Human Skeletal Remains." *International Journal of Legal Medicine* 132 (6): 1545–53. https://doi.org/10.1007/s00414-018-1794-8.

Andersen, Mikkel M., and David J. Balding. 2017. "How Convincing Is a Matching Y-Chromosome Profile?" *PLOS Genetics* 13 (11): e1007028. https://doi.org/10.1371/journal.pgen.1007028.

Andersen, Mikkel M., and Poul Svante Eriksen. 2019. *Disclapmix: Discrete Laplace Mixture Inference Using the EM Algorithm* (version 1.7.3). https://CRAN.R-project.org/package=disclapmix.

Andersen, Mikkel M., Poul Svante Eriksen, Helle Smidt Mogensen, and Niels Morling. 2015. "Identifying the Most Likely Contributors to a Y-STR Mixture Using the Discrete Laplace Method." *Forensic Science International: Genetics* 15 (March): 76–83. https://doi.org/10.1016/j.fsigen.2014.09.011.

Andronowski, Janna M., Amy Z. Mundorff, Isaac V. Pratt, Jon M. Davoren, and David M. L. Cooper. 2017. "Evaluating Differential Nuclear DNA Yield Rates and Osteocyte Numbers among Human Bone Tissue Types: A Synchrotron Radiation Micro-CT Approach." *Forensic Science International: Genetics* 28 (May): 211–18. https://doi.org/10.1016/j.fsigen.2017.03.002.

Ballantyne, Kaye N., Arwin Ralf, Rachid Aboukhalid, Niaz M. Achakzai, Maria J. Anjos, Qasim Ayub, Jože Balažic, et al. 2014. "Toward Male Individualization with Rapidly Mutating Y-Chromosomal Short Tandem Repeats." *Human Mutation* 35 (8): 1021–32. https://doi.org/10.1002/humu.22599.

Butler, Erin, and Richard Li. 2014. "Genetic Markers for Sex Identification in Forensic DNA Analysis." *Publications and Research*, August. https://academicworks.cuny.edu/jj_pubs/262.

"CODIS and NDIS Fact Sheet." n.d. Page. Federal Bureau of Investigation. Accessed July 10, 2021. https://www.fbi.gov/services/laboratory/biometric-analysis/codis/codis-and-ndis-fact-sheet.

D'Amato, Maria E., V. B. Bajic, and S. Davison. 2011. "Design and Validation of a Highly Discriminatory 10-Locus Y-Chromosome STR Multiplex System." *Forensic Science International: Genetics*, Haploid DNA markers in Forensic Genetics, 5 (2): 122–25. https://doi.org/10.1016/j.fsigen.2010.08.015.

D'Amato, Maria E., Mongi Benjeddou, and Sean Davison. 2009. "Evaluation of 21 Y-STRs for Population and Forensic Studies," December, 2.

D'Amato, Maria E., Liezle Ehrenreich, Kevin Cloete, Mongi Benjeddou, and Sean Davison. 2010. "Characterization of the Highly Discriminatory Loci DYS449, DYS481, DYS518, DYS612, DYS626, DYS644 and DYS710." *Forensic Science International: Genetics* 4 (2): 104–10. https://doi.org/10.1016/j.fsigen.2009.06.011.

Emery, M. V., K. Bolhofner, S. Winingear, R. Oldt, M. Montes, S. Kanthaswamy, J. E. Buikstra, L. C. Fulginiti, and A. C. Stone. 2020. “Reconstructing Full and Partial STR Profiles from Severely Burned Human Remains Using Comparative Ancient and Forensic DNA Extraction Techniques.” *Forensic Science International: Genetics* 46 (May): 102272. https://doi.org/10.1016/j.fsigen.2020.102272.

Gaudio, Daniel, Daniel M. Fernandes, Ryan Schmidt, Olivia Cheronet, Debora Mazzarelli, Mirko Mattia, Tadhg O’Keeffe, Robin N. M. Feeney, Cristina Cattaneo, and Ron Pinhasi. 2019. “Genome-Wide DNA from Degraded Petrous Bones and the Assessment of Sex and Probable Geographic Origins of Forensic Cases.” *Scientific Reports* 9 (1): 8226. https://doi.org/10.1038/s41598-019-44638-w.

Ge, Jianye, and Bruce Budowle. 2021. “Forensic Investigation Approaches of Searching Relatives in DNA Databases.” *Journal of Forensic Sciences* 66 (2): 430–43. https://doi.org/10.1111/1556-4029.14615.

Hares, Douglas R. 2012. “Expanding the CODIS Core Loci in the United States.” *Forensic Science International: Genetics* 6 (1): e52–54. https://doi.org/10.1016/j.fsigen.2011.04.012.

Hedman, J., C. Dufva, L. Norén, C. Ansell, L. Albinsson, and R. Ansell. 2011. “Applying a PCR Inhibitor Tolerant DNA Polymerase Blend in Forensic DNA Profiling.” *Forensic Science International: Genetics Supplement Series*, Progress in Forensic Genetics 14, 3 (1): e349–50. https://doi.org/10.1016/j.fsigss.2011.09.037.

Hooper, Kyle. 2007. “Plexor Application Notes: Real Power for Real-Time PCR.” *Promega Corporations*.

Jordan, Liz, and Richard Kurtz. 2010. “Optical Design of CFX96™ Real-Time PCR Detection System Eliminates the Requirement of a Passive Reference Dye,” 6.

Kasu, Mohaimin, Jamie Fredericks, Mischa Fraser, Christiaan Labuschagne, Mpasi Lesaoana, and Maria Eugenia D’Amato. 2019. “Novel Y-Chromosome Short Tandem Repeat Sequence Variation for Loci DYS710, DYS518, DYS385, DYS644, DYS612, DYS626, DYS504, DYS481, DYS447 and DYS449.” *International Journal of Legal Medicine* 133 (6): 1681–89. https://doi.org/10.1007/s00414-019-02056-7.

Kayser, Manfred. 2017. “Forensic Use of Y-Chromosome DNA: A General Overview.” *Hum Genet*, 15.

Kayser, Manfred, Ralf Kittler, Axel Erler, Minttu Hedman, Andrew C. Lee, Aisha Mohyuddin, S. Qasim Mehdi, et al. 2004. “A Comprehensive Survey of Human Y-Chromosomal Microsatellites.” *The American Journal of Human Genetics* 74 (6): 1183–97. https://doi.org/10.1086/421531.

Klavens, Adam, Dana D. Kollmann, Kelly M. Elkins, and Cynthia B. Zeller. 2020. “Comparison of DNA Yield and STR Profiles from the Diaphysis, Mid-Diaphysis, and Metaphysis Regions of Femur and Tibia Long Bones.” *Journal of Forensic Sciences* 66 (3): 1104–13. https://doi.org/10.1111/1556-4029.14657.

Kralik, Petr, and Matteo Ricchi. 2017. “A Basic Guide to Real Time PCR in Microbial Diagnostics: Definitions, Parameters, and Everything.” *Frontiers in Microbiology* 8. https://www.frontiersin.org/article/10.3389/fmicb.2017.00108.

“LoBind Protein or Genomic Microcentrifuge Tubes, Eppendorf®.” n.d. VWR. Accessed March 19, 2022. https://us.vwr.com/store/product/4675800/lobind-protein-or-genomic-microcentrifuge-tubes-eppendorf.

Luptáková, Lenka, Andrea Bábelová, Radoslav Omelka, Branislav Kolena, Mária Vondráková, and Mária Bauerová. 2011. “Sex Determination of Early Medieval Individuals through Nested PCR Using a New Primer Set in the SRY Gene.” *Forensic Science International* 207 (1): 1–5. https://doi.org/10.1016/j.forsciint.2010.08.012.

Miller, Kevin W. P, Barry L Brown, and Bruce Budowle. 2003. “The Combined DNA Index System.” *International Congress Series*, Progress in Forensic Genetics 9. Proceedings from the 19th International ISFG Congress held in Munster, Germany between 28 August and 1 September 2001, 1239 (January): 617–20. https://doi.org/10.1016/S0531-5131(02)00502-2.

Napper, Robin. 2000. “A National DNA Database the United Kingdom Experience.” *Australian Journal of Forensic Sciences* 32 (2): 65–69. https://doi.org/10.1080/00450610009410799.

Parsons, Thomas J., Rene M.L. Huel, Zlatan Bajunović, and Adnan Rizvić. 2019. “Large Scale DNA Identification: The ICMP Experience.” *Forensic Science International: Genetics* 38 (January): 236–44. https://doi.org/10.1016/j.fsigen.2018.11.008.

Phillips, Chris. 2018. “The Golden State Killer Investigation and the Nascent Field of Forensic Genealogy.” *Forensic Science International: Genetics* 36 (September): 186–88. https://doi.org/10.1016/j.fsigen.2018.07.010.

“PowerPlex® 21 System.” n.d. Accessed February 12, 2022. https://www.promega.com/products/forensic-dna-analysis-ce/str-amplification/powerplex-21-system/.

Quintana-Murci, Lluís, and Marc Fellous. 2001. “The Human Y Chromosome: The Biological Role of a ‘Functional Wasteland.’” *Journal of Biomedicine and Biotechnology* 1 (1): 18–24. https://doi.org/10.1155/S1110724301000080.

Roewer, Lutz. 2013. “DNA Fingerprinting in Forensics: Past, Present, Future.” *Investigative Genetics* 4 (1): 22. https://doi.org/10.1186/2041-2223-4-22.

———. 2019. “Y-Chromosome Short Tandem Repeats in Forensics—Sexing, Profiling, and Matching Male DNA.” *WIREs Forensic Science* 1 (4): e1336. https://doi.org/10.1002/wfs2.1336.

Rothstein, Mark A., and Meghan K. Talbott. 2006. “The Expanding Use of DNA in Law Enforcement: What Role for Privacy?” *The Journal of Law, Medicine & Ethics* 34 (2): 153–64. http://dx.doi.org/10.1111/j.1748-720X.2006.00024.x.

Science, National Research Council (US) Committee on DNA Technology in Forensic. 1992. *DNA Typing: Statistical Basis for Interpretation*. *DNA Technology in Forensic Science*. National Academies Press (US). https://www.ncbi.nlm.nih.gov/books/NBK234541/.

Shewale, Jaiprakash G., and Ray H. Liu. 2013. *Forensic DNA Analysis: Current Practices and Emerging Technologies*. CRC Press.

Siegert, Sabine, Lutz Roewer, and Michael Nothnagel. 2015. “Shannon’s Equivocation for Forensic Y-STR Marker Selection.” *Forensic Science International. Genetics* 16 (May): 216–25. https://doi.org/10.1016/j.fsigen.2015.02.001.

Siljic, Marina, Dubravka Salemovic, Valentina Cirkovic, Ivana Pesic-Pavlovic, Jovan Ranin, Marija Todorovic, Slobodan Nikolic, Djordje Jevtovic, and Maja Stanojevic. 2017. “Forensic Application of Phylogenetic Analyses - Exploration of Suspected HIV-1 Transmission Case.” *Forensic Science International. Genetics* 27 (March): 100–105. https://doi.org/10.1016/j.fsigen.2016.12.006.

Stray, J. E., and J. G. Shewale. 2010. “Extraction of DNA from Human Remains.” *Forensic Science Review* 22 (2): 177–85.
Syndercombe Court, Denise. 2021. “The Y Chromosome and Its Use in Forensic DNA Analysis.” Edited by Niamh Nic Daeid and Lucina Hackman. *Emerging Topics in Life Sciences* 5 (3): 427–41. https://doi.org/10.1042/ETLS20200339.
Tseng, Jennifer. 2008. “Sex, Gender, and Why the Differences Matter.” *AMA Journal of Ethics* 10 (7): 427–28. https://doi.org/10.1001/virtualmentor.2008.10.7.fred1-0807.
Wang, Chuan-Chao, Cosimo Posth, Anja Furtwängler, Katalin Sümegi, Zsolt Bánfai, Miklós Kásler, Johannes Krause, and Béla Melegh. 2021. “Genome-Wide Autosomal, MtDNA, and Y Chromosome Analysis of King Bela III of the Hungarian Arpad Dynasty.” *Scientific Reports* 11 (1): 19210. https://doi.org/10.1038/s41598-021-98796-x.
White, Tim. 2011. *Human Osteology*. 3rd ed. Academic Press.
Wyner, Nicole, Mark Barash, and Dennis McNevin. 2020. “Forensic Autosomal Short Tandem Repeats and Their Potential Association With Phenotype.” *Frontiers in Genetics* 11: 884. https://doi.org/10.3389/fgene.2020.00884.

Appendix I

Table 8: List of all sample locations, with bone type, weight of bone powder at time of extraction, extraction date, and Qubit™ reading.

Side	Bone	Location	Sample	Cortical or Trabecular	Weight (g)	Extract Date	Qubit™ (ng/µl)
Left	Clavicle	Lateral End	LC3	Cortical	0.055	3.27.22	0.000
Left	Clavicle	Lateral End	LC4	Trabecular	0.108	12.31.22	0.000
Right	Clavicle	Lateral End	CL3	Cortical	0.078	3.27.22	0.174
Right	Clavicle	Lateral End	CL4	Trabecular	0.078	3.17.22	0.540
Left	Femur	Nutrient Foramen	LFEM3	Cortical	0.078	3.27.22	0.000
Left	Femur	Nutrient Foramen	LFEM5	Trabecular	0.062	3.27.22	0.068
Left	Femur	Inter Condylar Fossa	LFEM6	Cortical	0.096	1.7.22	0.141
Left	Femur	Inter Condylar Fossa	LFEM7	Trabecular	0.065	3.17.22	0.000
Right	Femur	Nutrient Foramen	FEM3	Cortical	0.08	8.12.21	0.064
Right	Femur	Nutrient Foramen	FEM5	Trabecular	0.08	8.12.21	0.000
Right	Femur	Inter Condylar Fossa	FEM6	Cortical	0.15	8.12.21	0.302
Right	Femur	Inter Condylar Fossa	FEM7	Trabecular	0.13	8.12.21	0.000
Left	Fibula	Styloid Process	LFIB1	Cortical	0.057	3.27.22	0.000
Left	Fibula	Styloid Process	LFIB2	Trabecular	0.067	3.27.22	0.000
Right	Fibula	Styloid Process	FIB1	Cortical	0.078	3.27.22	0.000
Right	Fibula	Styloid Process	FIB2	Trabecular	0.062	3.27.22	0.117
Left	Humerus	Bicipital Groove	LH1	Cortical	0.068	3.27.22	0.000
Left	Humerus	Bicipital Groove	LH2	Trabecular	0.06	3.27.22	0.000
Left	Humerus	Deltoid Tuberosity	LH3	Cortical	0.062	3.27.22	0.000
Left	Humerus	Deltoid Tuberosity	LH5	Trabecular	0.069	3.27.22	0.088
Right	Humerus	Bicipital Groove	HUM1	Cortical	0.079	3.27.22	0.000
Right	Humerus	Bicipital Groove	HUM2	Trabecular	0.072	3.27.22	0.105
Right	Humerus	Deltoid Tuberosity	HUM3	Cortical	0.065	3.27.22	0.000
Right	Humerus	Deltoid Tuberosity	HUM5	Trabecular	0.08	3.27.22	0.000
Left	Metacarpal	3rd Metacarpal	LMC3A	Cortical	0.067	3.27.22	0.000
Left	Metacarpal	3rd Metacarpal	LMC3B	Trabecular	0.1	1.4.22	0.000
Right	Metacarpal	3rd Metacarpal	MC3A	Cortical	0.064	3.27.22	0.000
Right	Metacarpal	3rd Metacarpal	MC3B	Trabecular	0.075	3.18.22	0.315
Left	Metatarsal	2rd Metatarsal	LMT2A	Cortical	0.061	3.27.22	0.000
Left	Metatarsal	2th Metatarsal	LMT2B	Trabecular	0.109	1.4.22	0.000
Right	Metatarsal	3th Metatarsal	MT3A	Cortical	0.072	3.27.22	0.000
Right	Metatarsal	3th Metatarsal	MT3B	Trabecular	0.059	3.27.22	0.000
Left	Os Coxa	Ischial Tuberosity	LOS5	Cortical	0.065	3.27.22	0.000
Left	Os Coxa	Ischial Tuberosity	LOS6	Trabecular	0.067	3.27.22	0.000
Right	Os Coxa	Ischial Tuberosity	OS5	Cortical	0.078	3.27.22	0.000
Right	Os Coxa	Ischial Tuberosity	OS6	Trabecular	0.086	3.27.22	0.000
Left	Radius	Radial Head	LRAD1	Cortical	0.111	1.4.22	1.180

Left	Radius	Radial Head	LRAD2	Trabecular	0.071	3.27.22	0.097
Left	Radius	Radial Tuberosity	LRAD3	Cortical	0.062	3.27.22	0.000
Left	Radius	Radial Tuberosity	LRAD5	Trabecular	0.113	1.4.22	0.440
Right	Radius	Radial Head	RAD1	Cortical	0.086	3.25.22	0.000
Right	Radius	Radial Head	RAD2	Trabecular	0.1	1.14.22	0.000
Right	Radius	Radial Tuberosity	RAD3	Cortical	0.105	1.14.22	0.000
Right	Radius	Radial Tuberosity	RAD5	Trabecular	0.072	3.27.22	0.000
Left	Rib	Rib 1	LR1A	Cortical	0.1	1.7.22	0.060
Left	Rib	Rib 1	LR1B	Trabecular	0.08	1.7.22	0.000
Right	Rib	Rib 1	R1A	Cortical	0.073	3.27.22	0.579
Right	Rib	Rib 1	R1B	Trabecular	0.055	3.27.22	0.504
Left	Scapula	Glenoid Fossa	LSC1	Cortical	0.07	3.27.22	0.082
Left	Scapula	Glenoid Fossa	LSC2	Trabecular	0.073	3.28.22	0.683
Right	Scapula	Glenoid Fossa	GF1	Cortical	0.065	3.28.22	0.296
Right	Scapula	Glenoid Fossa	GF2	Trabecular	0.052	3.28.22	0.467
Left	Tibia	Tibial Plateau	LTIB1	Cortical	0.076	3.17.22	0.000
Left	Tibia	Tibial Plateau	LTIB2	Trabecular	0.106	1.7.22	0.000
Left	Tibia	Mid-Diaphysis	LTIB3	Cortical	0.079	3.28.22	0.000
Left	Tibia	Mid-Diaphysis	LTIB5	Trabecular	0.072	3.28.22	0.123
Right	Tibia	Tibial Plateau	TIB1	Cortical	0.06	8.12.21	0.661
Right	Tibia	Tibial Plateau	TIB2	Trabecular	0.13	8.12.21	0.298
Right	Tibia	Mid-Diaphysis	TIB3	Cortical	0.14	8.12.21	0.264
Right	Tibia	Mid-Diaphysis	TIB5	Trabecular	0.06	8.12.21	0.243
Left	Ulna	Olecranon Process	LU1	Cortical	0.072	3.28.22	0.059
Left	Ulna	Olecranon Process	LU2	Trabecular	0.061	3.28.22	0.000
Left	Ulna	Brachial Tuberosity	LU3	Cortical	0.0073	3.28.22	0.000
Left	Ulna	Brachial Tuberosity	LU5	Trabecular	0.061	3.28.22	0.000
Right	Ulna	Olecranon Process	U1	Cortical	0.079	3.25.22	0.000
Right	Ulna	Olecranon Process	U2	Trabecular	0.108	1.14.22	0.000
Right	Ulna	Brachial Tuberosity	U3	Cortical	0.12	1.14.22	0.073
Right	Ulna	Brachial Tuberosity	U5	Trabecular	0.065	3.25.22	0.000
Left	Temporal	Petrous Portion	LP	Trabecular	0.083	3.27.22	0.000
Right	Temporal	Petrous Portion	RP	Trabecular	0.08	3.25.22	0.000
Midline	C. Vertebrae	Body/Dens	C2A	Cortical	0.1	12.31.21	0.367
Midline	C. Vertebrae	Body	C2B	Trabecular	0.1	1.4.22	1.700
Midline	L. Vertebrae	Body	LV2A	Cortical	0.112	1.4.22	0.176
Midline	L. Vertebrae	Body	LV2b	Trabecular	0.1	12.31.21	0.000
Midline	T. Vertebrae	Body	T3A	Cortical	0.086	3.20.22	0.000
Midline	T. Vertebrae	Body	T3B	Trabecular	0.068	3.20.22	0.000
Midline	Sacrum	Sacral Promontory	SAC1	Cortical	0.059	3.28.22	0.000
Midline	Sacrum	Sacral Promontory	SAC2	Trabecular	0.073	3.28.22	0.000
Midline	Sternum	Distal Corpus Sterni	STE3	Cortical	0.067	3.28.22	0.000

Table 9: List of all samples with the qPCR results.

Side	Bone	Location	Cortical or Trabecular	Qubit (ng/µl)	Y-chromosome (ng/µl)	Autosomal (ng/µl)
Left	Clavicle	Lateral End	Cortical	0.174	0.06054	0.13830
Left	Clavicle	Lateral End	Trabecular	0.540	0.01082	0.08975
Right	Clavicle	Lateral End	Cortical	0.064	0.27307	0.64781
Right	Clavicle	Lateral End	Trabecular	0.000	0.00465	0.03534
Left	Femur	Nutrient Foramen	Cortical	0.302	0.08194	0.16600
Left	Femur	Nutrient Foramen	Trabecular	0.000	0.00332	0.03646
Left	Femur	Inter Condylar Fossa	Cortical	0.000	0.16343	0.47739
Left	Femur	Inter Condylar Fossa	Trabecular	0.117	0.01320	0.04574
Right	Femur	Nutrient Foramen	Cortical	0.000	0.30707	0.60443
Right	Femur	Nutrient Foramen	Trabecular	0.105	0.04026	0.12636
Right	Femur	Inter Condylar Fossa	Cortical	0.000	0.59377	1.53072
Right	Femur	Inter Condylar Fossa	Trabecular	0.000	0.00000	0.00337
Left	Fibula	Styloid Process	Cortical	0.000	0.01201	0.03816
Left	Fibula	Styloid Process	Trabecular	0.000	0.00168	0.00397
Right	Fibula	Styloid Process	Cortical	0.000	0.04271	0.09643
Right	Fibula	Styloid Process	Trabecular	0.068	0.01006	0.01359
Left	Humerus	Bicipital Groove	Cortical	0.141	0.00408	0.02671
Left	Humerus	Bicipital Groove	Trabecular	0.000	0.00796	0.03404
Left	Humerus	Deltoid Tuberosity	Cortical	0.000	0.05226	0.15069
Left	Humerus	Deltoid Tuberosity	Trabecular	0.000	0.00363	0.04568
Right	Humerus	Bicipital Groove	Cortical	0.000	0.00677	0.02307
Right	Humerus	Bicipital Groove	Trabecular	0.000	0.06299	0.26617
Right	Humerus	Deltoid Tuberosity	Cortical	0.000	0.04831	0.02974
Right	Humerus	Deltoid Tuberosity	Trabecular	0.088	0.00556	0.04154
Left	Metacarpal	3rd Metacarpal	Cortical	0.000	0.00625	0.02215
Left	Metacarpal	3rd Metacarpal	Trabecular	0.000	0.06446	0.27344
Right	Metacarpal	3rd Metacarpal	Cortical	0.000	0.00947	0.05444
Right	Metacarpal	3rd Metacarpal	Trabecular	0.000	0.00420	0.03476
Left	Metatarsal	2rd Metatarsal	Cortical	0.000	0.00504	0.01999
Left	Metatarsal	2th Metatarsal	Trabecular	0.000	0.01460	0.05681
Right	Metatarsal	3th Metatarsal	Cortical	1.180	0.01841	0.04524
Right	Metatarsal	3th Metatarsal	Trabecular	0.097	0.00442	0.01762
Left	Os Coxa	Ischial Tuberosity	Cortical	0.000	0.00972	0.04316
Left	Os Coxa	Ischial Tuberosity	Trabecular	0.440	0.00547	0.05825
Right	Os Coxa	Ischial Tuberosity	Cortical	0.000	0.00605	0.03402
Right	Os Coxa	Ischial Tuberosity	Trabecular	0.315	0.00405	0.04727
Left	Radius	Radial Head	Cortical	0.000	0.00000	0.00000
Left	Radius	Radial Head	Trabecular	0.000	0.04332	0.12991
Left	Radius	Radial Tuberosity	Cortical	0.000	0.09513	0.20431

Left	Radius	Radial Tuberosity	Trabecular	0.000	0.14771	0.64271
Right	Radius	Radial Head	Cortical	0.000	0.02790	0.08588
Right	Radius	Radial Head	Trabecular	0.000	0.06008	0.27063
Right	Radius	Radial Tuberosity	Cortical	0.000	0.01964	0.06167
Right	Radius	Radial Tuberosity	Trabecular	0.000	0.00272	0.04302
Left	Rib	Rib 1	Cortical	0.060	0.03231	0.11266
Left	Rib	Rib 1	Trabecular	0.000	0.00341	0.04044
Right	Rib	Rib 1	Cortical	0.579	0.03649	0.11375
Right	Rib	Rib 1	Trabecular	0.504	0.00584	0.01686
Left	Scapula	Glenoid Fossa	Cortical	0.082	0.13555	0.27374
Left	Scapula	Glenoid Fossa	Trabecular	0.683	0.00390	0.01384
Right	Scapula	Glenoid Fossa	Cortical	0.296	0.18945	0.73983
Right	Scapula	Glenoid Fossa	Trabecular	0.467	0.06433	0.36074
Left	Temporal	Petrous Portion	Trabecular	0.000	0.00705	0.02772
Right	Temporal	Petrous Portion	Trabecular	0.000	0.00619	0.01469
Left	Tibia	Tibial Plateau	Cortical	0.000	0.02436	0.06259
Left	Tibia	Tibial Plateau	Trabecular	0.000	0.00122	0.00380
Left	Tibia	Mid-Diaphysis	Cortical	0.000	0.00796	0.05063
Left	Tibia	Mid-Diaphysis	Trabecular	0.123	0.02369	0.04214
Right	Tibia	Tibial Plateau	Cortical	0.661	0.33054	1.41029
Right	Tibia	Tibial Plateau	Trabecular	0.298	0.01795	0.09577
Right	Tibia	Mid-Diaphysis	Cortical	0.264	0.43065	0.98559
Right	Tibia	Mid-Diaphysis	Trabecular	0.243	0.01143	0.01769
Left	Ulna	Olecranon Process	Cortical	0.059	0.12563	0.57870
Left	Ulna	Olecranon Process	Trabecular	0.000	0.01890	0.07079
Left	Ulna	Brachial Tuberosity	Cortical	0.000	0.07556	0.28048
Left	Ulna	Brachial Tuberosity	Trabecular	0.000	0.01024	0.04716
Right	Ulna	Olecranon Process	Cortical	0.000	0.01570	0.06890
Right	Ulna	Olecranon Process	Trabecular	0.000	0.10105	0.82193
Right	Ulna	Brachial Tuberosity	Cortical	0.073	0.01221	0.04884
Right	Ulna	Brachial Tuberosity	Trabecular	0.000	0.00575	0.02547
Midline	C. Vertebrae	Body/Dens	Cortical	0.367	0.20719	0.65028
Midline	C. Vertebrae	Body	Trabecular	1.700	0.02899	0.25968
Midline	L. Vertebrae	Body	Cortical	0.176	0.18860	0.54553
Midline	L. Vertebrae	Body	Trabecular	0.000	0.00283	0.01111
Midline	Sacrum	Sacral Promontory	Cortical	0.000	0.01431	0.03000
Midline	Sacrum	Sacral Promontory	Trabecular	0.000	0.00034	0.00203
Midline	Sternum	Distal Corpus Sterni	Cortical	0.000	0.00133	0.00292
Midline	T. Vertebrae	Body	Cortical	0.000	0.08560	0.28364
Midline	T. Vertebrae	Body	Trabecular	0.000	0.00245	0.00552

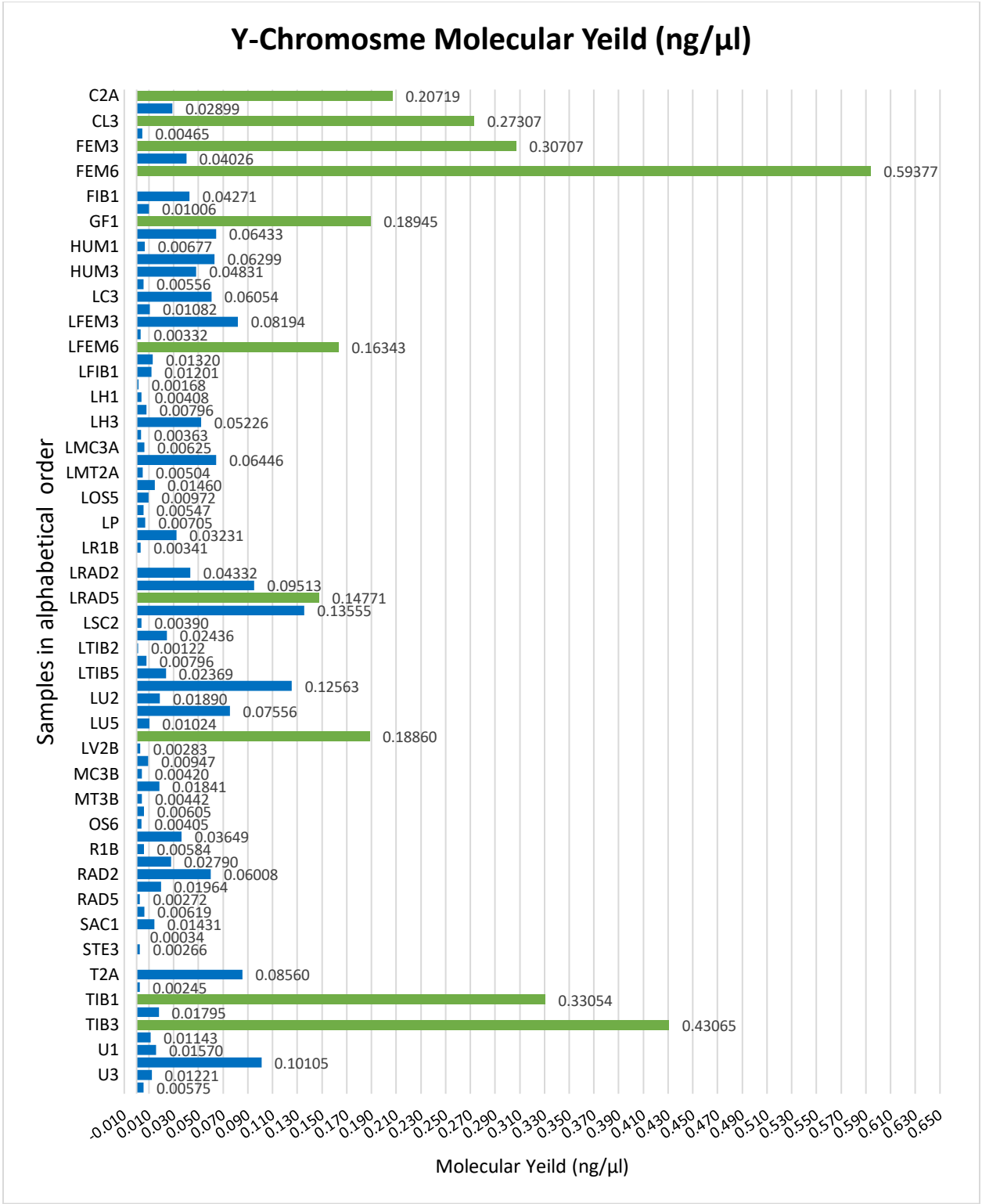

Figure 5: The Y-chromosome yield for all samples in alphabetical order. The top ten yields are indicated by the green bars.

Appendix II

Figure 6: Overview of remains pre- drilling.

Figure 7: The right humerus pre-drilling

Figure 8: Both the left and right humeri post-drilling

Figure 9: The left scapula pre-drilling.

Figure 10: Both the left and right scapula post-drilling.

Figure 11: Three of the Lumbar vertebrae pre-drilling.

Figure 12: Three of the Lumbar vertebrae post-drilling.

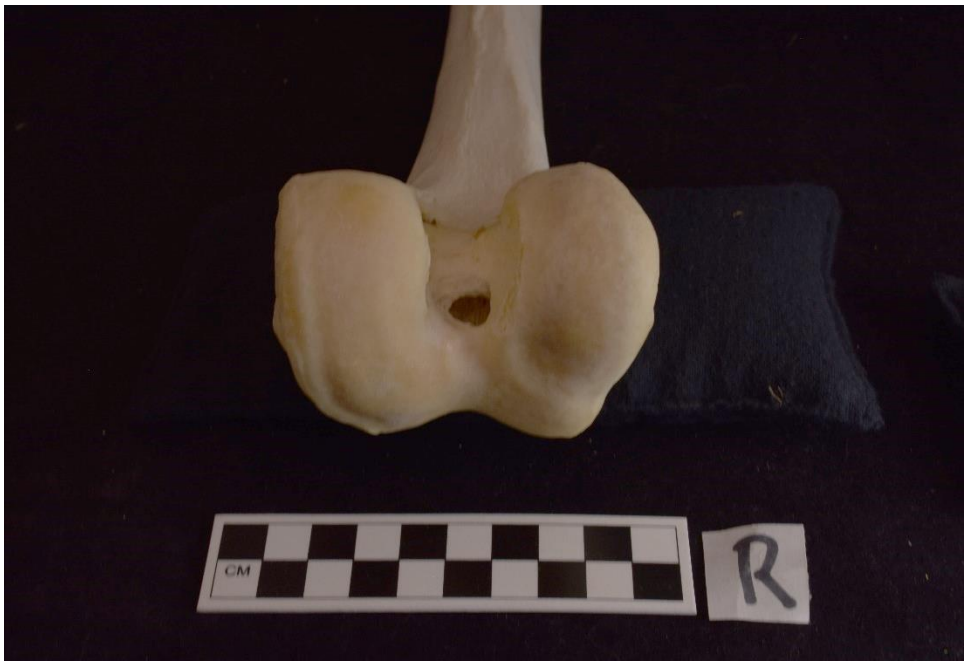

Figure 13: The intercondylar fossa of the right femur. Shows the overall good condition of the bone.

Figure 14: The tibial plateau of the left tibia. The sample was wet and dark brown due to unknown reasons when extracted.

Figure 15: The sacral promontory of the sacrum. Shows the bleached color produced by the overprocessing of the remains.